Marshall University
Marshall Digital Scholar

Biochemistry and Microbiology   Faculty Research

2-15-2013

Inhibition of Cholinergic Signaling Causes Apoptosis in Human Bronchioalveolar Carcinoma

Jamie K. Lau
Marshall University, lauj@marshall.edu

Kathleen C. Brown
Marshall University

Brent A. Thornhill
Marshall University, thornhill3@marshall.edu

Clayton M. Crabtree
Marshall University

Aaron M. Dom
Marshall University, dom@marshall.edu

See next page for additional authors

Follow this and additional works at: http://mds.marshall.edu/sm_bm

Part of the Biological Phenomena, Cell Phenomena, and Immunity Commons, and the Chemicals and Drugs Commons

Recommended Citation

Authors

Jamie K. Lau, Kathleen C. Brown, Brent A. Thornhill, Clayton M. Crabtree, Aaron M. Dom, Theodore R. Witte, W. Elaine Hardman, Christopher A. McNees, Cody A. Stover, A. Betts Carpenter, Haitao Luo, Yi C. Chen, Brandon S. Shiflett, and Piyali Dasgupta

Inhibition of cholinergic signaling causes apoptosis in human bronchioalveolar carcinoma

Jamie K. Lau[1][$], Kathleen C. Brown[1][$], Brent A. Thornhill[1][$], Clayton M. Crabtree[1], Aaron M. Dom[1], Theodore R. Witte[2], W. Elaine Hardman[2], Christopher A. McNees[1], Cody A. Stover[1], A. Betts Carpenter[3], Haitao Luo[4], Yi C. Chen[4], Brandon S. Shiflett[1], and Piyali Dasgupta[1*]

[1]Department of Pharmacology, Physiology, and Toxicology, Joan C. Edwards School of Medicine, Marshall University, Huntington, WV 25755

[2]Department of Biochemistry and Microbiology, Joan C. Edwards School of Medicine, Marshall University, Huntington, WV 25755

[3]Department of Anatomy and Pathology, Joan C. Edwards School of Medicine, Marshall University, Huntington, WV 25755

[4]Department of Biology, Alderson-Broaddus College, Philippi, WV 26416

*Correspondence to: Piyali Dasgupta, Department of Pharmacology, Physiology, and Toxicology, Joan C. Edwards School of Medicine, Marshall University, 1700 3rd Avenue, Huntington, WV 25755. E-mail: dasgupta@marshall.edu.

[$]These authors contributed equally to the work presented here and should therefore be regarded as equivalent authors.

The authors declare that they have no conflict of interest.

Abstract

Recent case-controlled clinical studies show that bronchioalveolar carcinomas (BACs) are correlated with smoking. Nicotine, the addictive component of cigarettes, accelerates cell proliferation through nicotinic acetylcholine receptors (nAChRs). In this study, we show that human BACs produce acetylcholine (ACh) and contain several cholinergic factors including acetylcholinesterase (AChE), choline acetyltransferase (ChAT), choline transporter 1 (CHT1, SLC5A7), vesicular acetylcholine transporter (VAChT, SLC18A3) and nACh receptors (AChRs, CHRNAs). Nicotine increased the production of ACh in human BACs and ACh acts as a growth factor for these cells. Nicotine-induced ACh production was mediated by α7-, α3β2-, and β3-nAChRs, ChAT and VAChT pathways. We observed that nicotine upregulated ChAT and VAChT. Therefore, we conjectured that VAChT antagonists, such as vesamicol, may suppress the growth of human BACs. Vesamicol induced potent apoptosis of human BACs in cell culture and nude mice models. Vesamicol did not have any effect on EGF or IGF-II-induced growth of human BAC's. siRNA-mediated attenuation of VAChT reversed the apoptotic activity of vesamicol. We also observed that vesamicol inhibited Akt phosphorylation during cell death, and overexpression of constitutively active Akt reversed the apoptotic activity of vesamicol. Taken together, our results suggested that disruption of nicotine-induced cholinergic signaling by agents such as vesamicol may have applications in BAC therapy.

KEY WORDS: Bronchioalveolar carcinoma, Acetylcholine, α7/β3 nAChR, VAChT, CHT1, Vesamicol, Akt

Précis

Findings that cholinergic signaling are critical to the survival of bronchioalveolar carcinoma cells should prompt immediate clinical testing of approved drugs that disrupt this pathway to determine if they can improve the efficacy of treatments for this form of lung cancer.

Introduction

Bronchioalveolar carcinoma (BAC) is a subtype of lung adenocarcinoma arising from type II pneumonocytes in the lung. The World Health Organization (WHO) revised its classification of BAC's in 2004 to include lung adenocarcinomas, which grow in a lepidic fashion along the alveolar septa without invasion into the stroma, pleura, blood vessels or lymphatics (1-3). The incidence of pure BAC is about 4%; however, mixed subtypes, including BACs with stromal invasion and pulmonary adenocarcinoma with BAC-like morphological features, account for almost 20% of all non-small cell lung cancers (NSCLC) (4). Cigarette smoking is the leading risk factor for the development of lung cancer. It is estimated that smoking is associated with 80-90% of lung cancer cases throughout the world (5). Smoking has a stronger association with small cell lung cancer (SCLC) than with adenocarcinoma (6). BAC is a relatively rare type of adenocarcinoma; therefore, only a few epidemiological studies have investigated the relationship between BAC and smoking (7-9).

Traditionally, the role of tobacco smoking in the etiology of human BAC originates from a series of early studies involving human lung cancer patients, most of which were non-smokers (1). These non-smoking lung cancer patients had higher incidence of BAC than other types of lung cancer. The resulting impression was that smoking is unimportant in the etiology of human BAC (1). However, these reports did not contain any cohort or case control studies that formally determined the relationship of human BACs to cigarette smoking.

Epidemiological data have demonstrated an association between human BACs and smoking (7, 8, 10). The risk of developing BACs is greater for people who started smoking at a younger age, smoked for a longer time or smoked more cigarettes per day. Conversely, the risk decreases in proportion to the duration of smoking cessation. Smoking habits have been correlated to both the mucinous and non-mucinous form of human BACs (11). Rolen et al., (2003) performed a case-control study and compared smoking status of 198 BAC patients to an equal number of controls. They observed that the risk of BAC is strongly related to the smoking

history of patients. They also found that both current and former smokers were at risk of developing BAC (9). Recently, Boffeta et al., (2011) analyzed seven case controlled studies in the USA comprising of 799 cases of BACs and 15,859 controls. They found that ever smokers are at a two-fold greater risk of developing lung BAC as compared to never smokers. They also observed a positive correlation between the duration and amount of smoking and the development of lung BAC (8).

Although cigarette smoke is comprised of a mixture of many compounds, nicotine is the addictive component of cigarette smoke (12). Several convergent studies have shown that nicotine promotes the progression of human BACs and confers resistance against chemotherapy (12, 13). All of these observations suggest that nicotine-induced mitogenic and pro-survival pathways contribute to the pathophysiology of BACs.

The proliferative activity of nicotine is mediated by nicotinic acetylcholine receptors (nAChRs) (12). The endogenous ligand for nAChRs is acetylcholine (ACh) (14). Recent studies have shown that nAChRs are present in non-neuronal tissues, including lung cancer cells, lung epithelial cells, endothelial cells and keratinocytes (12). Small cell lung cancers (SCLCs) and squamous cell carcinoma of the lung (SCC-L) express all components of the ACh autocrine loop, including acetylcholinesterase (AChE), choline acetyltransferase (ChAT), vesicular acetylcholine transporter (VAChT), choline transporter1 (CHT1), nAChRs and muscarinic acetylcholine receptors. SCLC and SCC-L cells secrete ACh, which promotes their proliferation (14-17). Song et al., (2008) found that the muscarinic receptor antagonist Darifenacin displayed anti-tumor activity in human SCC-L in both cell culture and nude mice models (15, 18). Such observations suggest that the cholinergic network may be a viable molecular target in the therapy of human lung cancer.

The present manuscript investigates whether the cholinergic loop exists in human BACs. We show that human BAC cell lines produce ACh and express cholinergic proteins. We also show for the first time that nicotine can amplify the components of the cholinergic loop in human

5

BACs. Nicotine increased the production of ACh in human BAC cell lines in a time- and dose-dependent manner. ACh acted as a growth factor for human BAC cells. Nicotine upregulated VAChT and ChAT expression in human BAC cells. We conjectured that nicotine-induced increase of VAChT levels may provide a viable molecular target in human BACs. The VAChT antagonist vesamicol induced robust apoptosis of human BAC cells in both cell culture and *in vivo* models. Vesamicol did not affect EGF or IGF-II-induced growth pathways in human BACs. This finding suggests that the pro-apoptotic activity of vesamicol is specific to the acetylcholine-signaling pathway in human BACs. The pro-apoptotic activity of vesamicol was mediated via suppression of Akt activation. The data presented in this paper characterizes the cholinergic system in human BACs and offers novel avenues for BAC therapy. The results of our experiments are relevant to BAC patients who are exposed to secondhand smoke or use nicotine-based cessation devices (e.g. patches and gums) to quit smoking.

Methods

Ethical use and care of laboratory animals.

Nude mice (Charles River Laboratories International, Inc., Wilmington, MA, USA) were acclimatized for one week. They were housed in autoclaved cages with *ad libitum* access to food and water in HEPA-filtered racks and closely monitored by animal facility staff. All procedures involving nude mice were conducted according to the Animal Care and Use Guidelines in a facility accredited by the Association for Assessment and Accreditation of Laboratory Animal Care (AAALAC) International and were approved by the Institutional Animal Care and Use Committee (IACUC) of the Joan C. Edwards School of Medicine, Marshall University (Protocol # 421).

Authentication of Cell lines

The human bronchioalveolar carcinoma (BAC) cell lines, A549, NCI-H358, and NCI-H650 (hereinafter referred to as A549, H358 and H650), and the human SCC-L cell line H520 were obtained from ATCC (Manassas, VA). The A549, H358 and H520 cells were authenticated by the ATCC Cell Authentication Service in October 2012. They used Short Tandem Repeat (STR) profiling for authentication of these cells, and the results are summarized in Supplementary Figure S1. The human BAC cell line H650 was passaged for less than six months and therefore did not require authentication. This cell line was obtained from ATCC which used STR profiling for its characterization. Primary human pulmonary alveolar epithelial cells (HPAEpiCs) were obtained from ScienCell (Carlsbad, CA). These cells were characterized by ScienCell using immunostaining for specific markers. A certificate of analysis was provided.

Cell Culture

A549 and H358 were cultured in RPMI-1640, supplemented with 2.0 mM glutamine, 100 units/mL penicillin, 50.0 μg/mL streptomycin, 1.0 mg/mL BSA, 1X insulin, transferrin, sodium selenite (ITS) supplement (Invitrogen Corp, Carlsbad, CA), 50 nM hydrocortisone and 1.0 μg/mL human EGF (15, 16). This medium will be referred to hereafter as serum-free RPMI (SF-RPMI). For a few experiments, the cells were rendered quiescent by incubating them in SF-RPMI containing ¼ ITS supplement, 12.5 nM hydrocortisone, 0.25 μg/mL EGF. This media, reduced serum-free RPMI, will be referred to hereafter as SF-RPMI-R. H650 was grown in a 1:1 mixture of DMEM and Ham's F-12K, supplemented with 2.0 mM L-glutamine, 100 units/mL penicillin, 50.0 μg/mL streptomycin, 0.02 mg/mL bovine insulin, 1X ITS, 50 nM hydrocortisone, 100 mM ethanolamine, 100 mM O-phosphorylethanolamine, 100 mM 3,3`,5-triiodo-L-thyronine, 5% (w/v) BSA, 0.5 mM sodium pyruvate, 10 mM HEPES, and 100 μg/mL EGF. The culture conditions for H520 and HPAEpiCs are described in Supplementary Methods.

Measurement of ACh production

A549 cells were grown in SF-RPMI. On the day of the assay, 100 μM neostigmine (an acetylcholinesterase inhibitor) was added to each plate (16). Four hours after the addition of neostigmine, the indicated doses of nicotine were added and the cells were incubated at 37°C for 36 hours. The supernatant was collected and spun at 800g. Subsequently, the supernatant was lyophilized, reconstituted with 1/5 volume autoclaved water, and stored at -80°C until further analysis. The amount of ACh in the sample was measured using the Choline/acetylcholine Quantification Kit (Biovision, Milpitas, CA, USA) (15-17). Each sample was assayed in triplicate, and the whole experiment was performed two independent times for each cell line.

Immunohistochemical staining of VAChT, ChAT in human BAC tissue microarray (TMA) and normal lung TMA

Human BAC tissue microarray slides (Abnova, Walnut, CA, USA) were deparaffinized and rehydrated as described previously (19, 20). The immunostaining was performed using Vectastain ABC Kit (Vector Laboratories, Burlingame, CA, USA) following the manufacturer's protocol. The dilutions of primary antibodies used were 1:50 (polyclonal VAChT antibody) and 1:25 (monoclonal ChAT antibody). The images were captured by phase contrast microscopy (Leica Microsystems, Wetzlar, Germany) at a magnification of 400X. The normal lung TMA (US Biomax Inc, Rockville, MD) was stained for VAChT and ChAT as described above.

VAChT, ChAT and nAChR ELISA assays

The concentration of VAChT and ChAT was measured using the VAChT ELISA Kit (Antibodies Online Inc., Atlanta, GA, USA) and the ChAT ELISA Kit (NovaTein Biosciences, Cambridge, MA), according to manufacturer's instructions. The expression of nAChR subunits in human BAC cell lines was analyzed by using α7-, α3-, β2- and β3- nAChR ELISA Kits

(Antibodies Online Inc.). Each of these assays was completed in duplicate, and the whole experiment was performed two independent times for each cell line.

TUNEL assays

A549 or H358 cells (10,000 cells/well) were seeded into an 8-well chamber slide in SF-RPMI and incubated overnight at 37°C (13, 19). Subsequently, the medium was replaced with SF-RPMI-R for 24 hours. After 24 hours, cells were treated with 100 nM nicotine in the presence or absence of 50 μM vesamicol. Cells were incubated for 48 hours at 37°C. Apoptosis was measured by the colorimetric TUNEL Assay (Promega Corporation, Madison, WI, USA), according to manufacturer's protocol. The magnitude of TUNEL-positive cells in the untreated control wells were considered to be equal to 1, and the TUNEL-positive cells in the remaining wells were calculated as fold-increase relative to the control. The experiment was performed two independent times with two replicates in each experiment.

Caspase-3 activity assay

Human BAC cells were incubated in SF-RPMI-R for 24 hours. Subsequently, cells were treated with 100 nM nicotine in the presence or absence of 50 μM vesamicol for 48 hours at 37°C. Lysates were made using the Caspase-3 Activity Kit (EMD Millipore Corporation, Billerica, MA, USA). Caspase-3 activity in untreated lysates was considered to be equal to 1, and the activity observed in treated lysates was calculated as fold-increase relative to the control cells. The experiment was performed two independent times with two replicates in each experiment.

Antitumor studies in nude mice

Four week-old male nude mice were acclimatized for one week and housed in autoclaved cages with *ad libitum* access to food and water in HEPA-filtered racks. A549 cells

were re-suspended in a 1:1 (v/v) solution of serum-free media and Matrigel matrix (BD Biosciences, San Jose, CA). One million cells were injected subcutaneously between the scapulae of each mouse (15, 21). After the tumors reached approximately 100 mm^3, the mice were randomized into two groups, a control (N=8) and a treatment (N=8) group. The control group was fed an AIN-76A based diet containing 10% corn oil. The treatment group was fed a diet containing 50 mg vesamicol/kg food, (approximately 10 mg vesamicol/kg body weight) per day. Both groups were administered nicotine in their drinking water (200 μg/mL in 2% saccharin sodium) (20, 21). The drug treatment was continued until tumors of the control group reached approximately 1500 mm^3. Mice were weighed once per week. Their food consumption and water consumption was monitored daily. Tumor lengths (l), widths (w) and height (h) were measured daily (6 days a week) for each mouse. Tumor volumes were calculated as (l x w x h)/2 (22, 23). After euthanizing the mice, the tumors were excised. Half of the tumor was snap frozen in liquid nitrogen. Tumor lysates were prepared using T-Per lysis buffer (Pierce Biotechnology, Rockford, IL), according to manufacturer's protocol (24). The other half of the tumor was fixed in 10% formalin buffered saline and used for immunohistochemistry.

Statistical analysis

All data was plotted using GraphPad Prism 5 Software, Inc (La Jolla, CA, USA), and was represented as the mean ± standard error of the mean (SEM). Results from the control and treated samples were compared using an analysis of variance followed by a Neumann-Keuls multiple comparison test. All analyses were completed using a 95% confidence interval. Data was considered significant when $p < 0.05$.

Results

Cholinergic proteins are expressed on bronchioalveolar carcinomas.

The cholinergic pathway proteins have been traditionally found in neuromuscular junctions and in neuronal cells (14). However, studies have shown that genes for these proteins are found in SCC-L and SCLC cells (14). ELISA experiments were performed to examine whether cholinergic proteins were expressed in human BAC cell lines and in HPAEpiCs. Figure 1A shows that multiple nAChR subunits are expressed on A549, H358 and H650 human BAC cells. Similarly, HPAEpiCs also expressed a diverse array of nAChR subunits. Immunoblotting experiments were performed to examine the presence of AChE, ChAT, CHT1 and VAChT (Figure 1B) in human BAC cell lines and in HPAEpiCs. H520 human SCC-L cells were used as the positive control for both of the experiments. We observed that human BAC cell lines, as well HPAEpiCs normal lung cells, express VAChT, ChAT, AChE and CHT1. The antibodies to VAChT, ChAT, CHT1 and AChE were found to be specific and showed only a single band at the correct molecular weight in full screen western blots (Supplementary Figure S2A-D). The expression of ChAT and VAChT was examined in human BAC tumors isolated from patients using BAC tissue microarray (TMA). The specific VAChT and ChAT antibodies described above were used for the immunostaining. Each TMA contained eighty-one samples of human BAC tumors from patients. Human BAC tumors displayed robust expression of both ChAT (Figure 1C; left panel) and VAChT (Figure 1D; right panel). Both VAChT and ChAT were found to be expressed in the cytoplasm. This observation is in agreement with previous data from several research groups showing that VAChT and ChAT are localized in the cytoplasm of cells (25-28). We also analyzed the expression of VAChT and ChAT in normal lung tissues using normal lung TMA (Supplementary Figure S3A-B). This TMA contained 20 samples of normal lung tissue. We found that normal lung tissues also express VAChT and ChAT, and these proteins are localized in the cytoplasm.

Nicotine induces acetylcholine production in bronchioalveolar carcinomas.

Next we wanted to assess the effect of nicotine on acetylcholine production in human BACs. We observed that nicotine increased ACh production from A549 cells in a concentration-dependent manner (Figure 2A). The maximum ACh production (2 μM) was observed at 100 nM nicotine and remained constant thereafter. A similar pattern was observed in H358 and H650 human BAC cells (Figure 2A). We also performed a time-kinetics experiment with nicotine on A549 cells and found that the maximal ACh production (2 μM) occurred at 36 hours and remained relatively constant thereafter (Figure 2B). Therefore, we selected a concentration of 100 nM nicotine and a 36 hour time point for all of our ACh production experiments. A point to note here is that 100 nM nicotine is within the concentration range found in the plasma of an average smoker (1 nM - 1 μM) (29).

Studies by Song et al., (2003) have demonstrated that ACh acts as an autocrine growth factor for SCLC cells (16, 17). We analyzed the mitogenic activity of ACh in human A549 BAC cells and found that ACh stimulated the proliferation of A549 cells in a concentration-dependent manner; the maximal proliferation observed at 2 μM ACh (Figure 2C: white bars). This finding is significant because the maximal mitogenic activity of ACh is similar to the amount of ACh secreted by human BACs. We repeated the BrdU cell proliferation assays in H358 human BAC cells and obtained similar results (Figure 2C: black bars). Our observations raise the possibility that nicotine induces the production of ACh in human BACs, which in turn, promotes the growth of human BACs in an autocrine manner.

Next, we wanted to determine the role of nAChRs in nicotine-induced ACh production. The treatment of A549 cells with the generalized nAChR antagonist mecamylamine (MCA) suppressed nicotinic-induced ACh production, whereas atropine, an antagonist to the closely related muscarinic receptor, had little to no effect on nicotine-induced ACh levels. We obtained

similar results in another human BAC cell line H358. Our results show that nicotine promotes ACh levels in human BACs in an nAChR dependent manner (Supplementary Figure S4A).

The next series of experiments aimed to investigate which specific nAChR subunits were responsible for nicotine-induced ACh production. Our data showed that the treatment of A549 and H358 human BAC cells with α7-nAChR subunit antagonists, methyllycaconitine (MLA) and α-bungarotoxin (α-BT), ablated nicotine-induced ACh production. Additionally, 1 µM of α-conotoxin MII (α-CT; α3β2 and β3 subunit antagonist) reversed the pro-secretory effect of nicotine, whereas DHβE (α3β2 and α4β2 nAChR antagonist) had little to no effect (Supplementary Figure S4B). Taken together, these results suggest that nicotine-induced ACh secretion is mediated via nAChRs, specifically through the α7-, α3β2- and β3-containing-nAChR subunits.

Finally, we wanted to examine the effect of choline/acetylcholine transporters on nicotine-induced ACh production. The treatment of A549 and H358 cells with hemicholinium (an antagonist of CHT1) suppressed nicotine-induced ACh secretion. Similarly, vesamicol (an antagonist of VAChT) potently abrogated nicotine-induced ACh production (Supplementary Figure S4C). Taken together, this shows that CHT1 and VAChT function are vital for nicotine-induced ACh production.

Nicotine increases VAChT and ChAT levels in human BAC cells.

We wanted to investigate whether nicotine promoted ACh secretion via the VAChT/ChAT pathway in BAC cells. We used an ELISA kit to measure VAChT and ChAT levels, which allowed us to quantitate these levels in an accurate and sensitive manner. We observed that the VAChT ELISA kit detected VAChT levels in asynchronous A549, H358, H650 BAC cells and HPAEpic normal lung cells (Supplementary Figure S5). The relative pattern of VAChT expression in the ELISA correlated well with the results obtained from western blotting

13

(Figure 1B; fourth panel). ELISA The treatment of A549 cells with 100 nM nicotine caused a 4-fold increase in VAChT levels (Figure 3A) and a 1.5-fold increases in ChAT levels (Figure 3B). Similarly, nicotine increased VAChT levels in H358 by 5.5-fold and ChAT levels by 1.4-fold (Figure 3A and 3B). We also tested the effect of nicotine on AChE and CHT1 in human BACs. We found that nicotine decreased AChE levels in H358 and A549 human BACs (Figure 3C). The levels of CHT1 were relatively unaffected by nicotine in both the cell lines (Figure 3C).

The VAChT antagonist vesamicol causes apoptosis in human BACs.

Our results showed that nicotine-induced ACh production was blocked by the VAChT inhibitor vesamicol (Supplementary Figure S4C). It may be envisaged that vesamicol will suppress nicotine-induced ACh production and thereby block ACh-induced growth of human BACs. Additionally, we conjectured that nicotine-induced upregulation of VAChT should provide a viable molecular target for vesamicol therapy in human BACs. MTT assays (Supplementary Methods online) demonstrated that vesamicol decreased the viability of nicotine-treated A549 and H358 human BAC lines in a concentration-dependent manner. The maximum reduction in cell viability was observed at 50 μM vesamicol (Figure 4A). Therefore, we used 50 μM vesamicol for all further experiments.

Next, we wanted to examine whether vesamicol induced apoptosis in human BAC cell lines. Quiescent A549 and H358 cells were treated with 100 nM nicotine in the presence or absence of 50 μM vesamicol. Apoptosis was measured by TUNEL assays. Figure 4B shows that vesamicol caused robust apoptosis in both A549 and H358 human BACs. The results of the TUNEL assays were verified by caspase-3 activity assay. We observed that vesamicol caused 2.5- to 3-fold increase in apoptosis relative to nicotine-treated human BAC cells (Figure 4C).

We also wanted to assess the effect of vesamicol on other mitogenic signaling pathways in human BACs (30-35). Several convergent studies indicate that EGF and IGF-II are potent

growth factors for human BAC cells (30-35). We performed a BrdU assay (Supplementary Methods online) to test the effect of vesamicol on EGF-induced proliferation of human BAC cell lines. We found that vesamicol has no effect on EGF-induced proliferation of A549 and H358 human BAC cell lines (Figure 4D). Similarly, vesamicol did not affect IGF-II-induced proliferation of human A549 and H358 cells (Figure 4E). Our findings seem to suggest that vesamicol specifically inhibits the acetylcholine-proliferative pathway in human BACs.

Vesamicol induces apoptosis in human BAC cells by specifically targeting VAChT

Vesamicol is a well characterized antagonist of VAChT (36). However, previous studies indicate that vesamicol also binds to the sigma-receptor in several types of human cancer cells (37, 38). We wanted to examine whether vesamicol induced apoptosis in human BAC cells by specifically targeting VAChT. For this purpose, we used siRNA methodology to suppress the expression of VAChT or sigma receptor in A549 cells. A549 cells were transfected with VAChT-siRNA or sigma-receptor-siRNA (Supplementary Methods Online). Eighteen hours post transfection, the cells were rendered quiescent by incubating them in SF-RPMI-R medium for 24 hours (19). Subsequently, the cells were treated with 100nM nicotine in the presence or absence of 50 μM vesamicol for 48 hours at 37°C. A549 cells transfected with a non-targeting control-siRNA was used as the negative control for the experiment. After 48 hours cell lysates were made and vesamicol-induced apoptosis was measured by the caspase-3 activity assay.

We observed that vesamicol-induced apoptosis was decreased upon transfection of VAChT-siRNA and unaffected by sigma-receptor-siRNA. The apoptotic activity of vesamicol was also unaffected by the control non-targeting siRNA (Figure 5A). We repeated these experiments in H358 human BAC cells and obtained similar results (Figure 5B). These experiments were also repeated with a second independent VAChT-siRNA (Ambion Inc., Grand Island, NY) and similar results were obtained (Figure 5C and D).

Parallel transfection experiments were performed to test the efficacy of VAChT-siRNA and sigma-receptor-siRNA in A549 cells. ELISA assays show that the levels of VAChT are robustly suppressed upon transfection with both sets of VAChT-siRNA (Supplementary Figure S6A and S6B) in A549 and H358 human BAC cells. Western blotting experiments show that the levels of sigma receptor are ablated upon transfection of sigma-receptor-siRNA (Supplementary Figure S6C and S6D) in both A549 and H358 cells.

We also examined whether vesamicol was targeting the VAChT pathway at concentrations lower than 50µM. We chose 10µM and 25µM vesamicol for our experiments. Caspase-3 activity assays show that the cellular apoptosis induced by 10µM vesamicol was suppressed by two independent sets of VAChT-siRNA in both A549 and H358 cells (Supplementary Figure S7A and S7B). Similarly, the transfection of VAChT-siRNA efficiently abrogated the apoptotic activity of 25µM vesamicol in nicotine-treated A549 and H358 cells (Supplementary Figure S7C and S7D). ELISA assays indicate that both the VAChT-siRNA decreased the expression of VAChT in A549 and H358 cells (Supplementary Figure S7E). Taken together, our data show that vesamicol caused apoptosis in human BAC cells by specifically targeting the VAChT pathway.

Vesamicol-induced apoptosis is mediated by the Akt pathway in human BACs.

The Akt signaling pathway plays a vital role in nAChR signaling in normal lung cells and lung cancer cells (12). We observed that the treatment of A549 and H358 human BAC cells with nicotine and vesamicol caused potent decreases in phosphorylated-Akt levels (Figure 6A and B). The levels of both phosphorylated-Akt (Thr308) and phosphorylated-Akt (Ser473) are robustly suppressed upon vesamicol treatment, whereas total Akt levels remain constant (Figure 6A and 6B, respectively). Western blotting analysis also showed that vesamicol had little to no effect on the expression of phosphorylated-Akt in untreated A549 (or H358) cells (Figure 6C and 6D). The transfection of constitutively active Akt (pcDNA3-HA-Akt-CA; Supplementary

Methods Online) reversed the apoptotic effect of vesamicol, demonstrating that vesamicol induces cell death by suppressing Akt activation (Figure 6E and 6F). Western blotting analysis confirms the over expression of HA-tagged Akt in A549 and H358 human BAC lines upon transfection (Supplementary Fig. S8A and S8B).

Vesamicol inhibited the growth of human A549 cells *in vivo*.

The anti-tumor activity of vesamicol was examined *in vivo* using a nude mice model (15, 21). A549 human BAC cells were injected between the scapulae of nude mice. The tumors were allowed to grow until approximately 100 mm^3, after which they were randomized into two groups. The control group was administered nicotine in the drinking water. The "vesamicol group" was administered 50 mg vesamicol/kg food along with nicotine. Our results showed that the administration of vesamicol decreased the tumor growth rate of A549 human BAC tumors (Figure 7A). The administration of 50 mg vesamicol/kg food in the diet was well tolerated and caused no discomfort or weight loss in mice (mean control = 25.6 ± 0.6 g; mean vesamicol treated = 25.2 ± 0.5 g). Additionally, food intake (mean control = 6.2 ± 0.04 g/day; mean vesamicol-treated = 6.2 ± 0.04 g/day) and water consumption (mean control = 11.0 ± 0.4 mL/day; mean vesamicol-treated = 11.2 ± 0.3 mL/day) was similar between groups.

H and E staining of the tumors revealed the presence of apoptotic bodies in the tumors belonging to the vesamicol-treated mice (Figure 7B). Caspase-3 activity assays indicate that tumor lysates from vesamicol-treated mice displayed about 2.5-fold greater apoptosis relative to control nicotine-treated mice (Figure 7C). Our data from cell culture suggested that vesamicol induced apoptosis by suppression of Akt activation. We wanted to investigate whether vesamicol-treated tumors had lower levels of phosphorylated-Akt. Western blotting analysis revealed that vesamicol-treated tumors had substantially lower levels of phosphorylated-Akt (Thr308 and Ser 473) relative to nicotine-treated A549 tumors (Figure 7D; top two panels). The total Akt levels were similar in all four pairs of tumors (Figure 7D; third panel from the top).

Taken together, these data indicate that vesamicol decreases tumor growth rates of A549 human BAC tumors *in vivo* by inducing robust apoptosis via an Akt-dependent pathway.

Discussion

Our study shows for the first time that human BACs produce ACh and contain a functional acetylcholine-signaling system. A functional cholinergic loop has also been detected in SCLCs, SCC-Ls and normal bronchial epithelial cells (14). Most importantly, nicotine regulates the cholinergic machinery and increases ACh levels by about 10-fold in human BACs. Nicotine upregulates the levels of cholinergic proteins, namely VAChT and ChAT, and concomitantly downregulates AChE in human BACs. Nicotine-induced increases of VAChT and ChAT promote ACh content and its transport into the extracellular environment. On the other hand, nicotine decreases AChE levels, which in turn suppress ACh degradation. Thus, the enhanced levels of ACh provide proliferative stimuli to human BACs. The amplification of the cholinergic network by nicotine offers novel therapeutic strategies for BAC therapy. These phenomena are highly significant since about 30% of lung cancer patients continue to smoke, use nicotine-based cessation patches or gum, or are exposed to environmental tobacco smoke after their diagnosis (39-41).

We observed that nicotine caused a 3-fold increase in VAChT and ChAT levels in human BAC cells. This led us to hypothesize that antagonists of VAChT should attenuate nicotine-induced ACh production and thereby suppress the growth of human BACs. As a "proof-of-principle" we decided to use the well-characterized VAChT antagonist, vesamicol, for our experiments. Our hypothesis was supported by the results of Song et al., (2003) who showed that vesamicol suppressed the growth of H82 human SCLC cells *in vitro*. We believe that our results are the first to report characterizing the anti-cancer activity of VAChT antagonists in human BAC using both cell culture and *in vivo* model systems. We found that vesamicol induced robust apoptosis in human BAC cells in both cell culture and *in vivo* systems.

A survey of literature shows that only very few studies have evaluated the anti-tumor activity of vesamicol. Ogawa et al., (2009) evaluated radioiodinated vesamicol analogs for tumor imaging and anti-tumor activity (42, 43). They found that radioiodinated-vesamicol-analogs suppressed the growth of human prostate cancer cells in mice model. However, their results showed that vesamicol exerted its anti-tumor activity by binding to the sigma receptor on DU145 prostate cancer cells (42). Several convergent studies have shown that vesamicol is also a ligand for the sigma-receptor. However, our experiments involving VAChT-siRNA and sigma-receptor-siRNA showed that the anti-cancer activity of vesamicol was specifically mediated by VAChT. It is possible that sigma-receptors do not play a vital role in nicotine-induced proliferative signaling in human BAC cells.

The present manuscript shows that apoptotic effects of vesamicol are mediated via suppression of the Akt pathway. Clinical studies have shown that the activation of Akt is highly prevalent in human BAC tumors. Nicotine causes rapid activation of Akt and its downstream substrates. Studies by West et al., (2001) have speculated that inhibition of the Akt pathway may be a viable strategy for treatment of tobacco-related lung cancers (44, 45). The EGFR inhibitors Gefitinib and Erlotinib have been shown to suppress Akt phosphorylation in human lung cancer cells (46, 47). Similarly, PI-3kinase/Akt inhibitors, i.e. LY294002 and deregulin, suppress proliferation of human BAC cells *in vitro* and in mouse models of tobacco carcinogenesis (48). Our results suggest that VAChT-antagonists such as vesamicol are another class of therapeutic agents capable of inhibiting activated Akt in human BACs.

The acetylcholine-signaling pathway has been found to regulate multiple cellular functions, such as proliferation, cell-to-cell contact, differentiation and cytoskeletal integrity (14). Apart from lung cancer cells, endothelial cells, mesothelial cells, immune cells and keratinocytes have been found to synthesize, transport and degrade acetylcholine (14). The pharmacological manipulation of this non-neuronal cholinergic system by agents, such as vesamicol, could lead

to the development of novel therapies for multiple tobacco-related diseases including lung cancer.

References

1. Levy BP, Drilon A, Makarian L, Patel AA, Grossbard ML. Systemic approaches for multifocal bronchioloalveolar carcinoma: is there an appropriate target? Oncology (Williston Park). 2010;24:888-98, 900.

2. Saintigny P, Wistuba, II, Kim ES. Bronchioloalveolar carcinoma: a translational perspective. Oncology (Williston Park). 2010;24:907-8, 14.

3. Colby TV, Noguchi M, Henschke C, Vazquez MF, Geisinger K, Yokose T.et al. Adenocarcinoma. In: Travis WD, Brambilla E, Muller-Hermelink HK, Harris CC et al., editors. World health classification of tumours pathology and genetics of tumours of the lung, pleura, thymus and heart. Lyon, France: IARC Press; 2004. p. 35-44.

4. Ebbert JO, Chhatwani L, Aubry MC, Wampfler J, Stoddard S, Zhang F, et al. Clinical features of bronchioloalveolar carcinoma with new histologic and staging definitions. J Thorac Oncol. 2010;5:1213-20.

5. The Health Consequences of Smoking. A report of the Surgeon General's Office on Smoking and Health, DHHS, Washington DC. 2004.

6. Cancer IARC. IARC Monographs on the Evaluation of Carcinogenic Risks to Humans. Tobacco Smoke and Involuntary Smoking: IARC, Lyon, France; 2004. p. 51-1187.

7. Garfield D. Mucinous and nonmucinous bronchioloalveolar carcinoma and smoking. Am J Clin Pathol. 2010;133:341-2.

8. Boffetta P, Jayaprakash V, Yang P, Asomaning K, Muscat JE, Schwartz AG, et al. Tobacco smoking as a risk factor of bronchioloalveolar carcinoma of the lung: pooled analysis of seven case-control studies in the International Lung Cancer Consortium (ILCCO). Cancer Causes Control. 2011;22:73-9.

9. Rolen KA, Fulton JPT, D. J., Strauss GM. Bronchoalveolar carcinoma (BAC) of the lung is related to cigarette smoking: A case-control study from Rhode Island (RI). 2003 ASCO Annual Meeting; 2003.

10. Morabia A, Wynder EL. Relation of bronchioloalveolar carcinoma to tobacco. BMJ. 1992;304:541-3.

11. Sartori G, Cavazza A, Sgambato A, Marchioni A, Barbieri F, Longo L, et al. EGFR and K-ras mutations along the spectrum of pulmonary epithelial tumors of the lung and elaboration of a combined clinicopathologic and molecular scoring system to predict clinical responsiveness to EGFR inhibitors. Am J Clin Pathol. 2009;131:478-89.

12. Singh S, Pillai S, Chellappan S. Nicotinic acetylcholine receptor signaling in tumor growth and metastasis. J Oncol. 2011;2011:456743.

13. Dasgupta P, Kinkade R, Joshi B, Decook C, Haura E, Chellappan S. Nicotine inhibits apoptosis induced by chemotherapeutic drugs by up-regulating XIAP and survivin. Proc Natl Acad Sci U S A. 2006;103:6332-7.

14. Song P, Spindel ER. Basic and clinical aspects of non-neuronal acetylcholine: expression of non-neuronal acetylcholine in lung cancer provides a new target for cancer therapy. J Pharmacol Sci. 2008;106:180-5.

15. Song P, Sekhon HS, Fu XW, Maier M, Jia Y, Duan J, et al. Activated cholinergic signaling provides a target in squamous cell lung carcinoma. Cancer Res. 2008;68:4693-700.

16. Song P, Sekhon HS, Jia Y, Keller JA, Blusztajn JK, Mark GP, et al. Acetylcholine is synthesized by and acts as an autocrine growth factor for small cell lung carcinoma. Cancer Res. 2003;63:214-21.

17. Song P, Sekhon HS, Proskocil B, Blusztajn JK, Mark GP, Spindel ER. Synthesis of acetylcholine by lung cancer. Life Sci. 2003;72:2159-68.

18. Song P, Sekhon HS, Lu A, Arredondo J, Sauer D, Gravett C, et al. M3 muscarinic receptor antagonists inhibit small cell lung carcinoma growth and mitogen-activated protein kinase phosphorylation induced by acetylcholine secretion. Cancer Res. 2007;67:3936-44.

19. Dasgupta P, Rizwani W, Pillai S, Davis R, Banerjee S, Hug K, et al. ARRB1-mediated regulation of E2F target genes in nicotine-induced growth of lung tumors. J Natl Cancer Inst. 2011;103:317-33.

20. Brown KC, Lau JK, Dom AM, Witte TR, Luo H, Crabtree CM, et al. MG624, an alpha7-nAChR antagonist, inhibits angiogenesis via the Egr-1/FGF2 pathway. Angiogenesis. 2012;15:99-114.

21. Brown KC, Witte TR, Hardman WE, Luo H, Chen YC, Carpenter AB, et al. Capsaicin displays anti-proliferative activity against human small cell lung cancer in cell culture and nude mice models via the E2F pathway. PLoS One. 2010;5:e10243.

22. Tomayko MM, Reynolds CP. Determination of subcutaneous tumor size in athymic (nude) mice. Cancer Chemother Pharmacol. 1989;24:148-54.

23. Shabbir M, Thompson CS, Mikhailidis D, Morgan RJ, Burnstock G. Extracellular ATP attenuates the growth of hormone refractory prostate cancer in vivo. Eur Urology Supplements. 2003;2:24-7.

24. Kinkade R, Dasgupta P, Carie A, Pernazza D, Carless M, Pillai S, et al. A small molecule disruptor of Rb/Raf-1 interaction inhibits cell proliferation, angiogenesis, and growth of human tumor xenografts in nude mice. Cancer Res. 2008;68:3810-8.

25. Schafer MK, Weihe E, Erickson JD, Eiden LE. Human and monkey cholinergic neurons visualized in paraffin-embedded tissues by immunoreactivity for VAChT, the vesicular acetylcholine transporter. J Mol Neurosci. 1995;6:225-35.

26. Tayebati SK, Tomassoni D, Di Stefano A, Sozio P, Cerasa LS, Amenta F. Effect of choline-containing phospholipids on brain cholinergic transporters in the rat. Journal of the neurological sciences. 2011;302:49-57.

27. Papka RE, Traurig HH, Schemann M, Collins J, Copelin T, Wilson K. Cholinergic neurons of the pelvic autonomic ganglia and uterus of the female rat: distribution of axons and presence of muscarinic receptors. Cell Tissue Res. 1999;296:293-305.

28. Takahara Y, Maeda M, Nakatani T, Kiyama H. Transient suppression of the vesicular acetylcholine transporter in urinary bladder pathways following spinal cord injury. Brain Res. 2007;1137:20-8.

29. Heeschen C, Jang JJ, Weis M, Pathak A, Kaji S, Hu RS, et al. Nicotine stimulates angiogenesis and promotes tumor growth and atherosclerosis. Nature Medicine. 2001;7:833-9.

30. Wilson KJ, Gilmore JL, Foley J, Lemmon MA, Riese DJ, 2nd. Functional selectivity of EGF family peptide growth factors: implications for cancer. Pharmacology & therapeutics. 2009;122:1-8.

31. Siegfried JM. Detection of human lung epithelial cell growth factors produced by a lung carcinoma cell line: use in culture of primary solid lung tumors. Cancer Res. 1987;47:2903-10.

32. Domingo G, Perez CA, Velez M, Cudris J, Raez LE, Santos ES. EGF receptor in lung cancer: a successful story of targeted therapy. Expert Rev Anticancer Ther. 2010;10:1577-87.

33. Linnerth NM, Baldwin M, Campbell C, Brown M, McGowan H, Moorehead RA. IGF-II induces CREB phosphorylation and cell survival in human lung cancer cells. Oncogene. 2005;24:7310-9.

34. Camidge DR, Dziadziuszko R, Hirsch FR. The rationale and development of therapeutic insulin-like growth factor axis inhibition for lung and other cancers. Clin Lung Cancer. 2009;10:262-72.

35. Dziadziuszko R, Camidge DR, Hirsch FR. The insulin-like growth factor pathway in lung cancer. J Thorac Oncol. 2008;3:815-8.

36. Bahr BA, Parsons SM. Acetylcholine transport and drug inhibition kinetics in Torpedo synaptic vesicles. J Neurochem. 1986;46:1214-8.

37. Wilke RA, Mehta RP, Lupardus PJ, Chen Y, Ruoho AE, Jackson MB. Sigma receptor photolabeling and sigma receptor-mediated modulation of potassium channels in tumor cells. J Biol Chem. 1999;274:18387-92.

38. Efange SM, Mach RH, Smith CR, Khare AB, Foulon C, Akella SK, et al. Vesamicol analogues as sigma ligands. Molecular determinants of selectivity at the vesamicol receptor. Biochem Pharmacol. 1995;49:791-7.

39. Johnson BE. Tobacco and lung cancer. Prim Care. 1998;25:279-91.

40. Johnson BE, Cortazar P, Chute JP. Second lung cancers in patients successfully treated for lung cancer. Semin Oncol. 1997;24:492-9.

41. Johnston-Early A, Cohen MH, Minna JD, Paxton LM, Fossieck BE, Jr., Ihde DC, et al. Smoking abstinence and small cell lung cancer survival. An association. Jama. 1980;244:2175-9.

42. Ogawa K, Shiba K, Akhter N, Yoshimoto M, Washiyama K, Kinuya S, et al. Evaluation of radioiodinated vesamicol analogs for sigma receptor imaging in tumor and radionuclide receptor therapy. Cancer Sci. 2009;100:2188-92.

43. Ogawa K, Kanbara H, Shiba K, Kitamura Y, Kozaka T, Kiwada T, et al. Development and evaluation of a novel radioiodinated vesamicol analog as a sigma receptor imaging agent. EJNMMI research. 2012;2:54.

44. West KA, Brognard J, Clark AS, Linnoila IR, Yang X, Swain SM, et al. Rapid Akt activation by nicotine and a tobacco carcinogen modulates the phenotype of normal human airway epithelial cells. J Clin Invest. 2003;111:81-90.

45. West KA, Linnoila IR, Belinsky SA, Harris CC, Dennis PA. Tobacco carcinogen-induced cellular transformation increases activation of the phosphatidylinositol 3'-kinase/Akt pathway in vitro and in vivo. Cancer Res. 2004;64:446-51.

46. Kitazaki T, Soda H, Doi S, Nakano H, Nakamura Y, Kohno S. Gefitinib inhibits MUC5AC synthesis in mucin-secreting non-small cell lung cancer cells. Lung Cancer. 2005;50:19-24.

47. Ko JC, Ciou SC, Jhan JY, Cheng CM, Su YJ, Chuang SM, et al. Roles of MKK1/2-ERK1/2 and phosphoinositide 3-kinase-AKT signaling pathways in erlotinib-induced Rad51 suppression and cytotoxicity in human non-small cell lung cancer cells. Mol Cancer Res. 2009;7:1378-89.

48. Denlinger CE, Rundall BK, Jones DR. Inhibition of phosphatidylinositol 3-kinase/Akt and histone deacetylase activity induces apoptosis in non-small cell lung cancer in vitro and in vivo. J Thorac Cardiovasc Surg. 2005;130:1422-9.
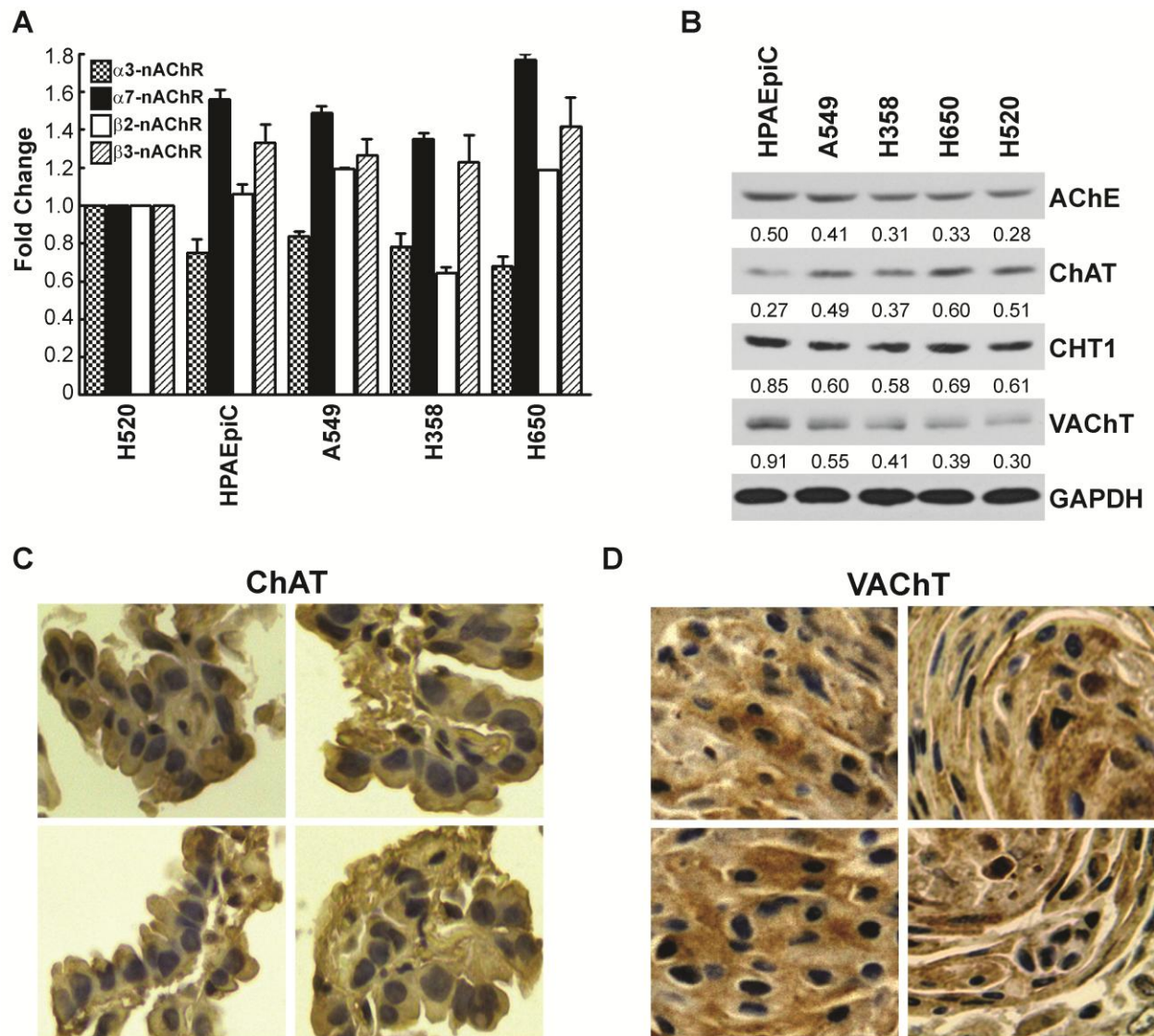
Figure 1. Human BACs and normal human alveolar epithelial cells (HPAEpiCs) express cholinergic proteins. **(A)** ELISA assays show that human BAC cell lines and HPAEpiCs express multiple nAChR subunits. The assay was completed in duplicate, and the whole experiment was performed two independent times. Results indicated by a different letter are significantly different ($P < 0.05$). **(B)** HPAEpiCs and human BACs express AChE, ChAT, CHT1 and VAChT. H520 human SCC-L cells were used as the positive control for the experiments outlined in (A) and (B). GAPDH was used as the loading control, and the results were quantitated by

densitometric analysis. The experiment was repeated twice, and the representative data is shown. **(C)** and **(D)** Immunohistochemistry of the human BAC microarray showed that BAC tumors (isolated from patients) express ChAT and VAChT in the cytoplasm, adjacent to the hemotoxylin-counterstained dark nuclei in the tissue samples. A tumor microarray containing 81 cores of human BACs was used for these experiments and four panels of representative photos are shown. Scale bar = 20 µm.
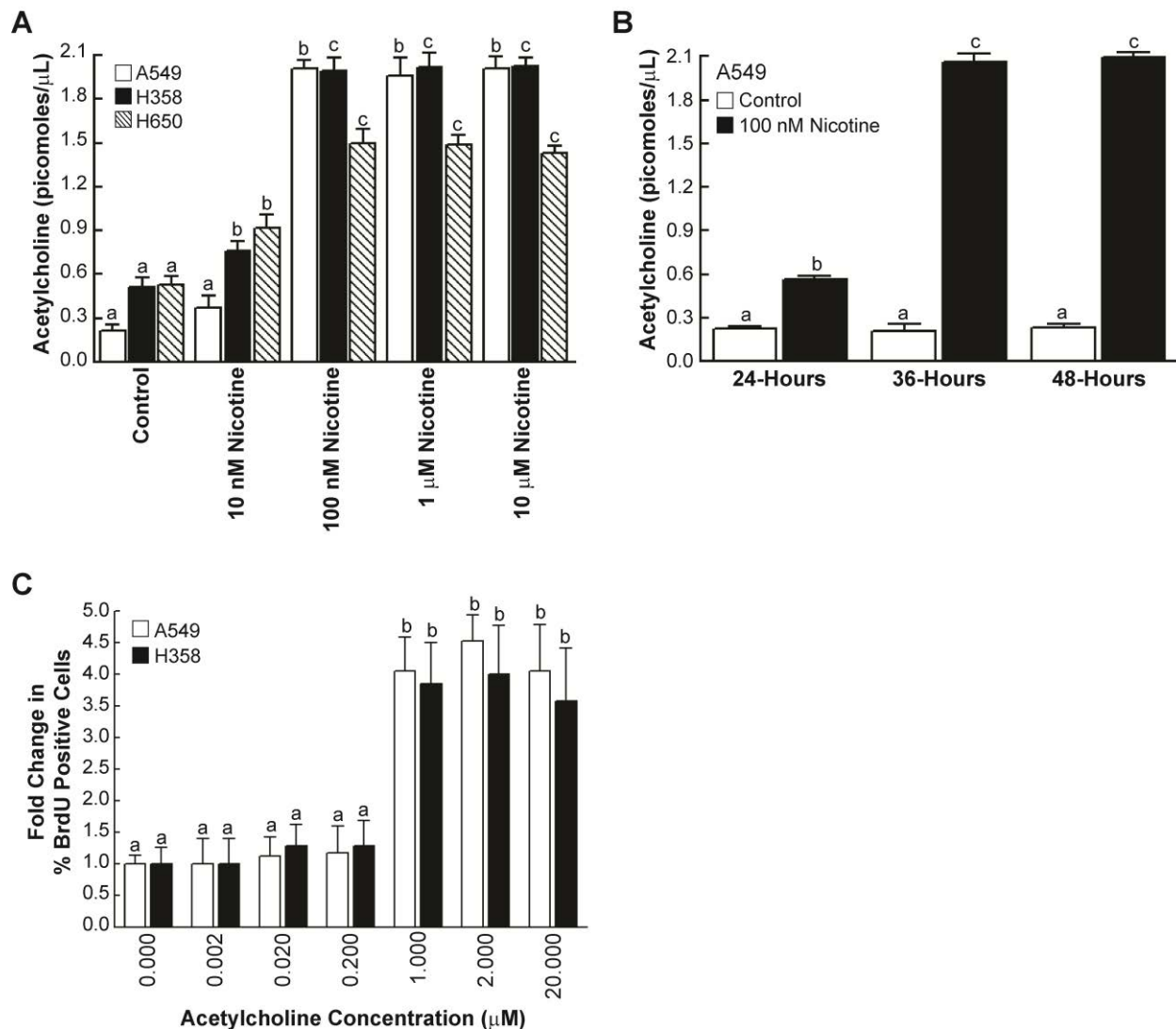
Figure 2. Nicotine induces the production of the growth factor ACh in human BACs. **(A)** Nicotine caused a concentration-dependent increase in ACh production in A549, H358 and H650 human BAC cell lines. **(B)** Time kinetics of nicotine-induced ACh production in A549 human BAC cells. The maximal ACh production was observed at 100 nM nicotine at 36 hours. **(C)** ACh stimulated proliferation of A549 and H358 cells. BrdU assays show that 2 μM of ACh (which is approximately the amount of ACh produced in nicotine-treated BAC cells) caused a 4- to 4.5-fold increase in proliferation of A549 and H358 human BACs. Each sample was analyzed in triplicate. Data represent mean $\pm$ SEM from two independent experiments. Results indicated by a different letter are significantly different ($P < 0.05$).
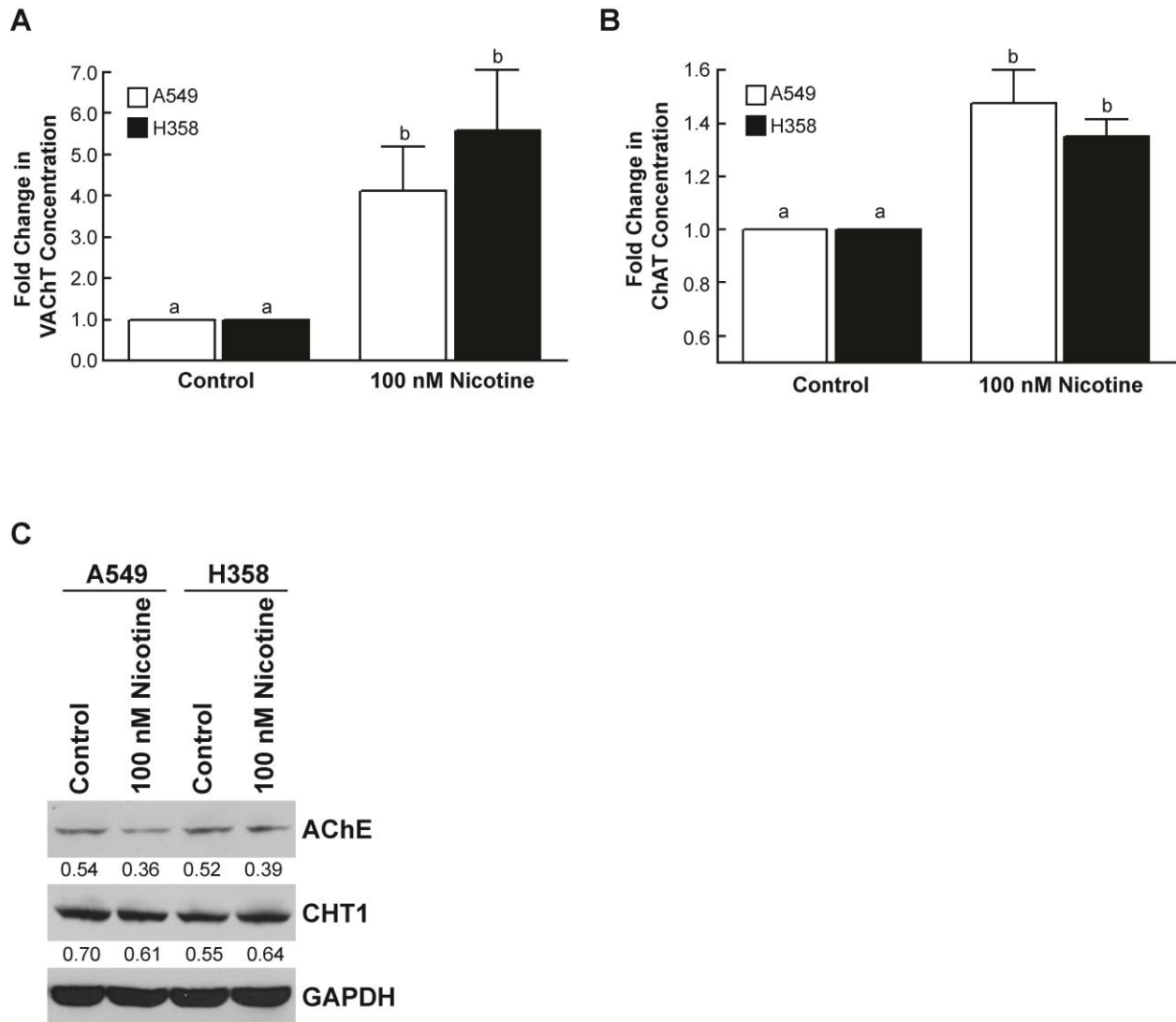
Figure 3. Effect of nicotine on cholinergic proteins in human BACs. **(A)** The treatment of A549 and H358 cells with 100 nM nicotine caused 4- to 5-fold increase in VAChT levels. **(B)** Nicotine produces a modest increase in ChAT levels. **(C)** Nicotine decreases AChE levels in both A549 and H358 cells. The levels of CHT1 are relatively unaffected by nicotine in human BAC cells. Data represent mean $\pm$ SEM from two independent experiments. Each sample was analyzed in triplicate. Results indicated by a different letter are significantly different ($P < 0.05$).
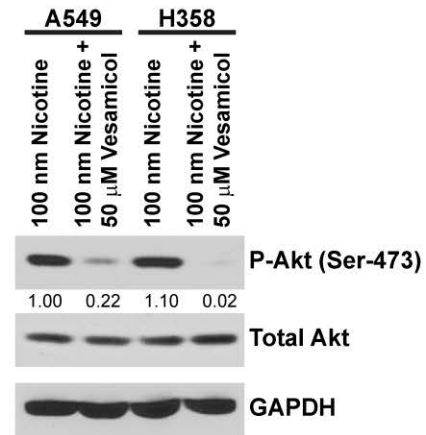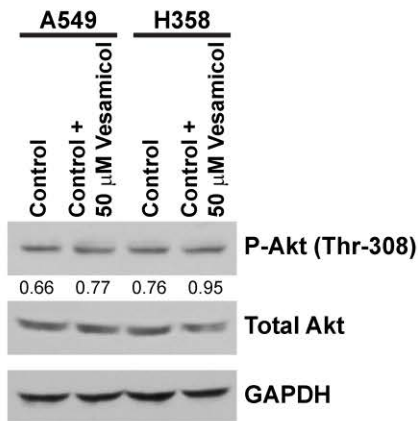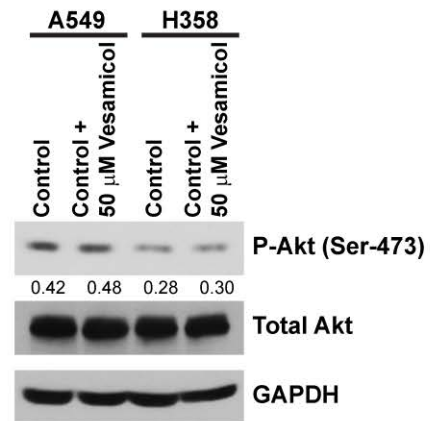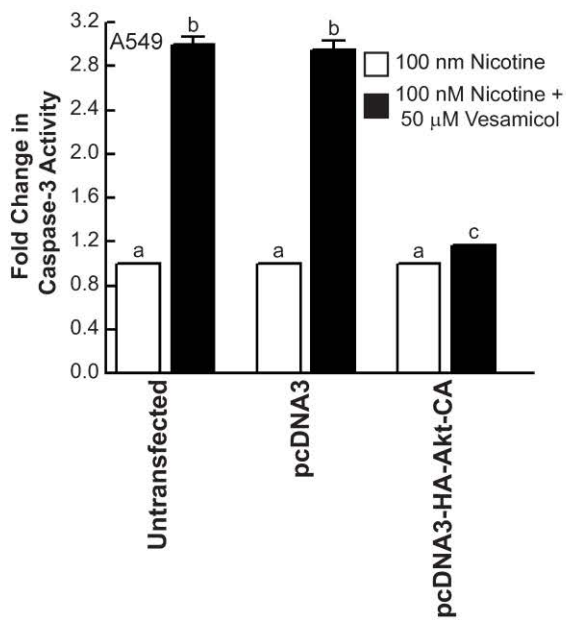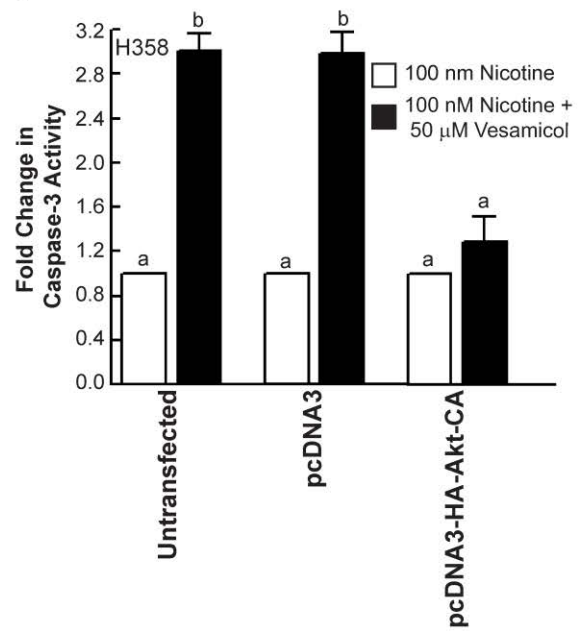
31
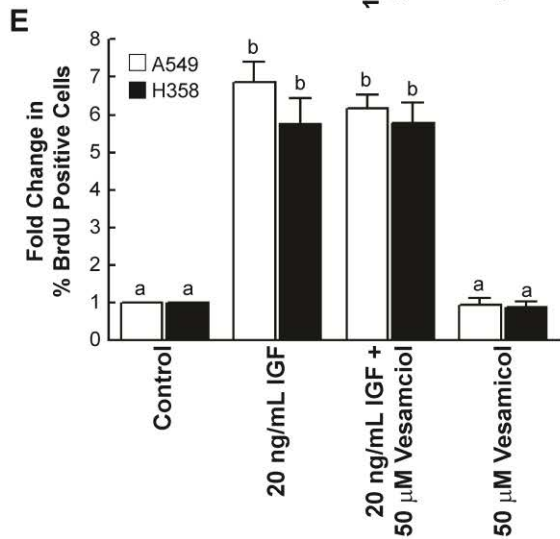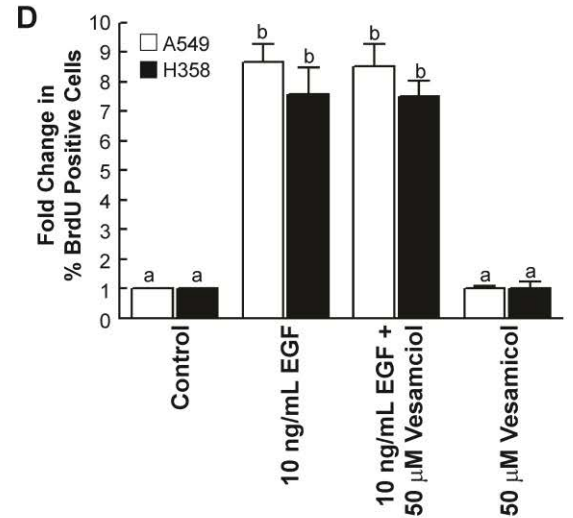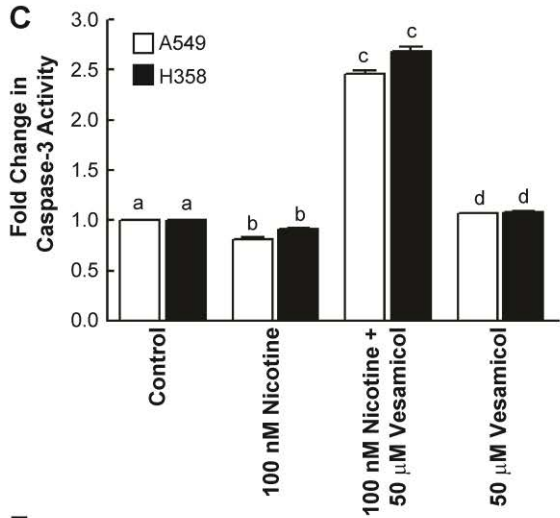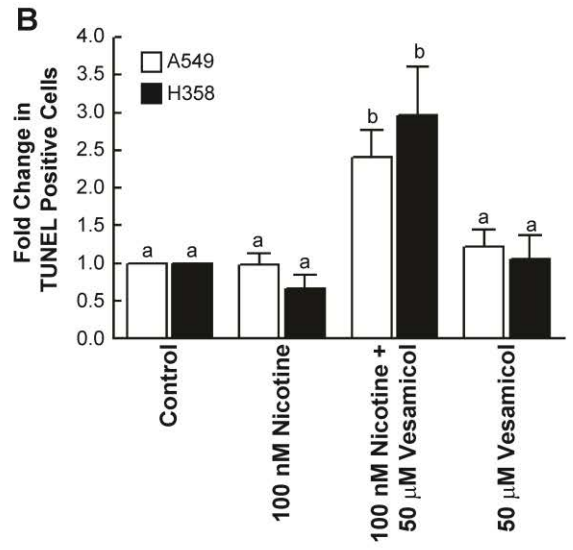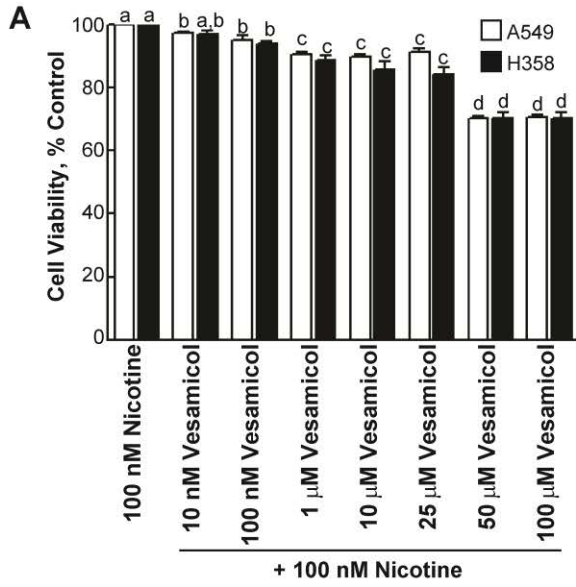
Figure 4. Vesamicol caused apoptosis in human BAC cells. **(A)** MTT assays showed that vesamicol decreases the viability of A549 and H358 cells in a concentration-dependent manner. Each sample was analyzed in triplicate. **(B)** The treatment of human BAC cell lines with 50 µM vesamicol caused 2.5- to 3-fold apoptosis in nicotine-treated A549 and H358 cells. **(C)** The apoptotic activity of vesamicol was confirmed with caspase-3 activity assay and similar results were obtained. **(D)** Vesamicol had no effect on EGF-induced proliferation of A549 and H358 cells. BrdU assays show that the treatment of A549 and H358 human BAC cells with 10 ng/ml EGF causes robust proliferation. The addition of 50 µM vesamicol along with EGF produced no effect on EGF-induced proliferation of human BACs. **(E)** BrdU assays demonstrate that vesamicol does not suppress IGF-II-induced proliferation of human BAC cell lines. Each sample was analyzed in duplicate. Data represent mean $\pm$ SEM from two independent experiments. Results indicated by a different letter are significantly different ($P < 0.05$).
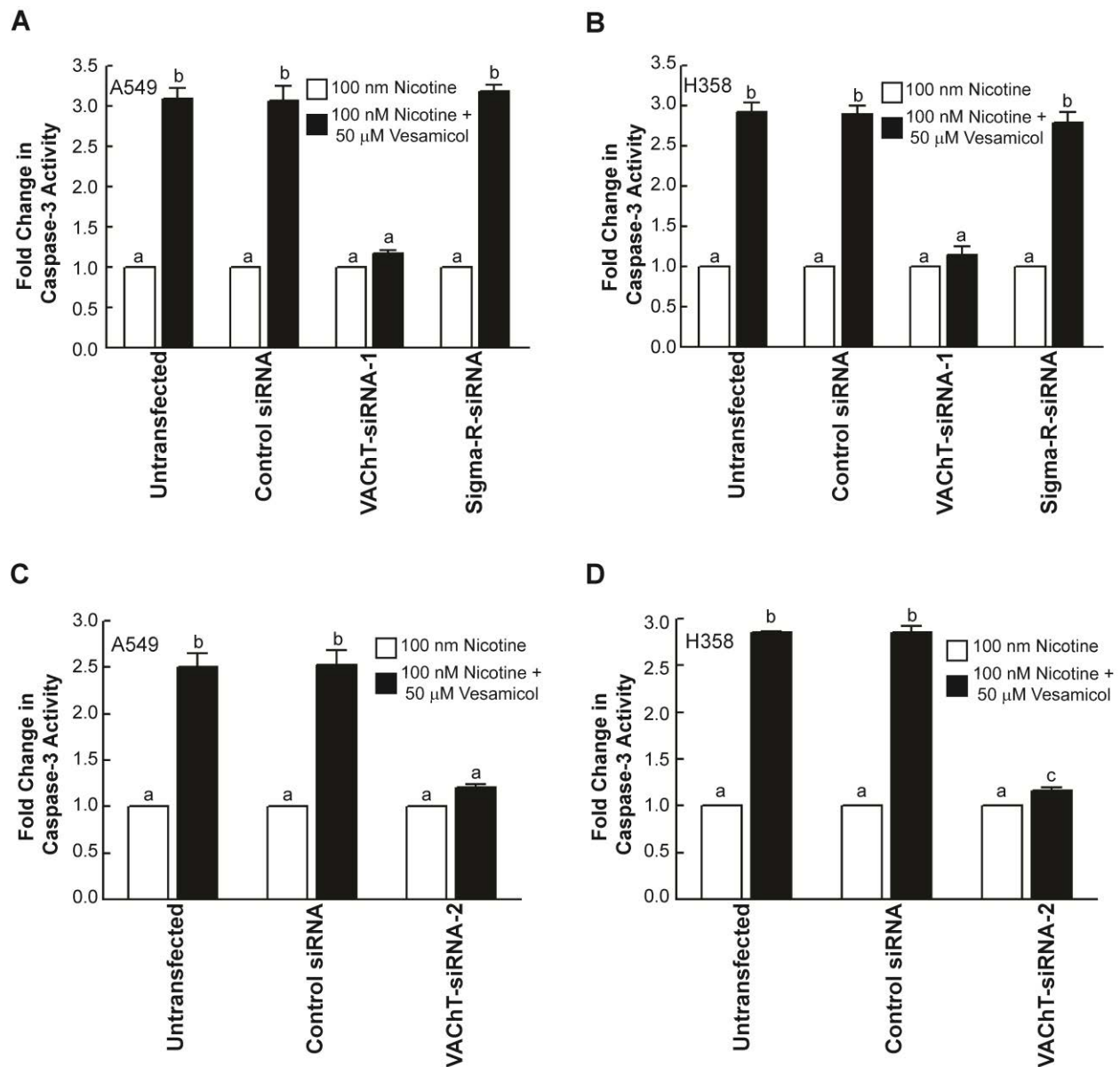
Figure 5. Vesamicol-induced apoptosis is specifically mediated by VAChT in human BAC cells.
(A) Caspase-3 activity assays showed that the transfection of VAChT-siRNA reversed vesamicol-induced apoptosis in nicotine-treated A549 cells, whereas transfection of sigma-receptor-siRNA (SigmaR-siRNA) or control-siRNA has no effect. **(B)** The experiment was repeated in H358 human BAC cells, and similar results were obtained. **(C)** The suppression of VAChT, with another independent VAChT-siRNA (VAChT-siRNA-2), abrogated vesamicol-induced apoptosis in A549 human BAC cells. **(D)** The experiment was repeated in H358 cells,

and similar results were obtained. Each sample was analyzed in duplicate. Data represent mean $\pm$ SEM from two independent experiments. Results indicated by a different letter are significantly different ($P < 0.05$).

A

A549   H358

100 nm Nicotine | 100 nm Nicotine + 50 μM Vesamicol | 100 nm Nicotine | 100 nm Nicotine + 50 μM Vesamicol

P-Akt (Thr-308)

0.88   0.41   0.98   0.15

Total Akt

GAPDH

B

A549   H358

100 nm Nicotine | 100 nm Nicotine + 50 μM Vesamicol | 100 nm Nicotine | 100 nm Nicotine + 50 μM Vesamicol

P-Akt (Ser-473)

1.00   0.22   1.10   0.02

Total Akt

GAPDH

C

A549   H358

Control | Control + 50 μM Vesamicol | Control | Control + 50 μM Vesamicol

P-Akt (Thr-308)

0.66   0.77   0.76   0.95

Total Akt

GAPDH

D

A549   H358

Control | Control + 50 μM Vesamicol | Control | Control + 50 μM Vesamicol

P-Akt (Ser-473)

0.42   0.48   0.28   0.30

Total Akt

GAPDH

E

A549

Fold Change in Caspase-3 Activity

□ 100 nm Nicotine
■ 100 nM Nicotine + 50 μM Vesamicol

Untransfected   pcDNA3   pcDNA3-HA-Akt-CA

F

H358

Fold Change in Caspase-3 Activity

□ 100 nm Nicotine
■ 100 nM Nicotine + 50 μM Vesamicol

Untransfected   pcDNA3   pcDNA3-HA-Akt-CA

35

Figure 6. The apoptotic activity of vesamicol is mediated by the Akt pathway. **(A)** The treatment of A549 and H358 human BAC cells with nicotine and vesamicol inhibited Akt phosphorylation at Thr-308. **(B)** Vesamicol decreased the levels of phospho-Akt (Ser-473) in nicotine-treated A549 and H358 cells. **(C)** Vesamicol had no effect on the levels of phospho-Akt (Thr-308) in untreated A549 and H358 cells. **(D)** The treatment of quiescent A549 and H358 cells 50 µM vesamicol does not affect phospho-Akt (Ser-473) levels. **(E)** The transfection of pcDNA3-HA-Akt-CA (T308D, S473D) reverses the apoptotic activity of vesamicol, whereas transfection of the empty vector had no effect on vesamicol-induced apoptosis in A549 human BAC cells. **(F**) The transfection experiment was repeated in H358 cells and similar results were obtained. Data represent mean $\pm$ SEM from two independent experiments. Each sample was analyzed in duplicate. Results indicated by a different letter are significantly different (P < 0.05).
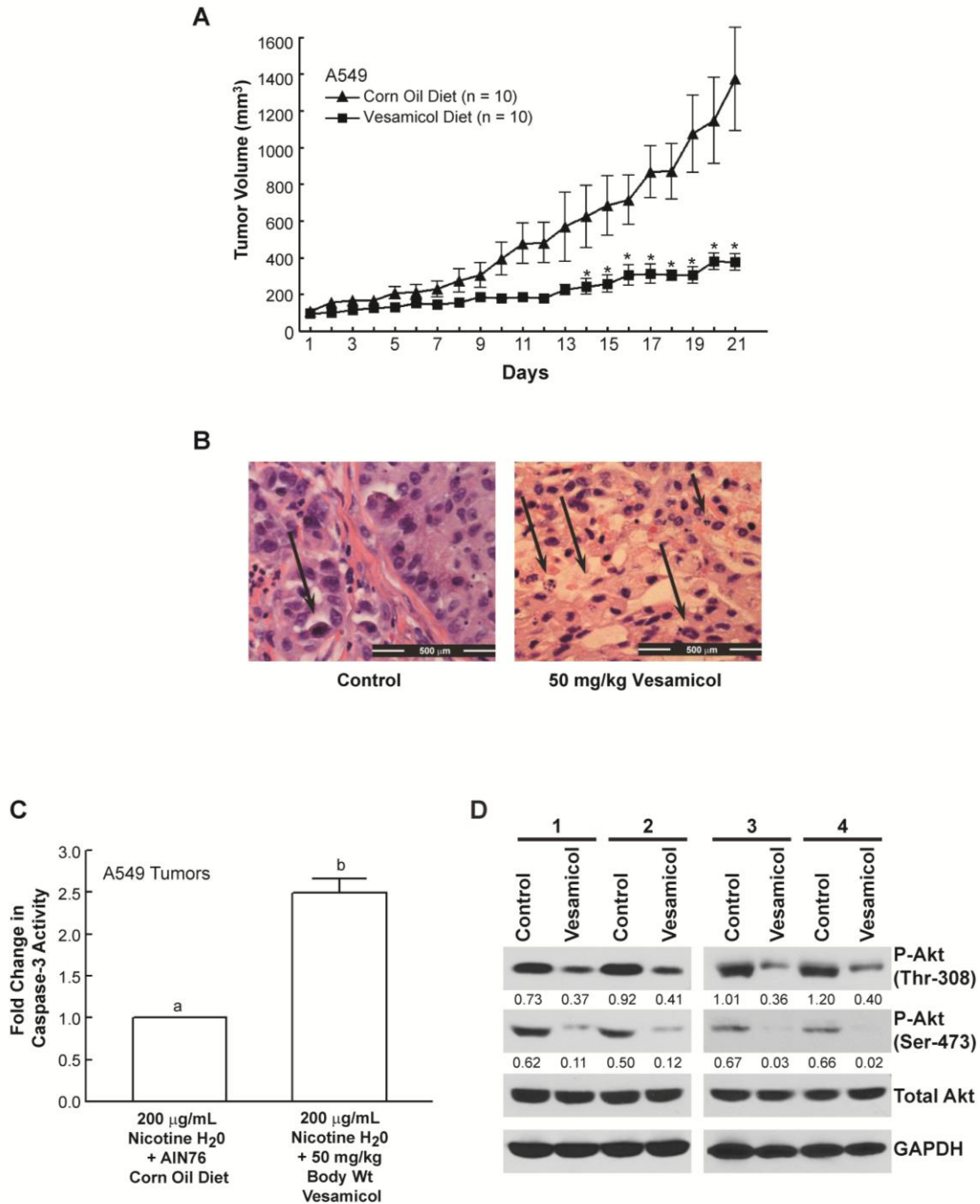
Figure 7. Vesamicol induces apoptosis of human BAC tumors *in vivo*. **(A)** The administration of

vesamicol (50 mg vesamicol/kg food) decreased the growth rate of A549 human BAC tumors

xenografted in nude mice. The nude mice experiments comprised of eight mice per group. **(B)**

The tumors from the mice were excised and stained with H & E. The black arrow shows the

presence of apoptotic bodies in the tissue sections. The vesamicol-treated tumors (right panel)

showed a greater number of apoptotic bodies relative to the mice administered vehicle (left panel). Scale bar = 500 μm. **(C)** An aliquot of the tumors from nude mice were frozen and lysates were made. Caspase-3 activity of these lysates was measured. The vesamicol-treated tumors had higher caspase-3 activity (indicating higher apoptosis) than the tumors in the control group. **(D)** Western blotting analysis showed that vesamicol-treated tumors showed lower levels of phospho-Akt (Thr308) and phospho-Akt (Ser473). The western blot was quantitated using NIH ImageJ 1.46p. Data represent mean $\pm$ SEM. Results indicated by a different letter or an asterisk are significantly different ($P < 0.05$).

Supplementary Methods

Reagents, Antibodies and Constructs

Nicotine, α-bungarotoxin (α-BT, α7-nAChR antagonist), dihydro-β-erythroidine hydrobromide (DHβE, α4β4- and α4β2-nAChR antagonist), hemicholinium (ChAT antagonist) and EGF were purchased from Sigma-Aldrich (St. Louis, MO). Acetylcholine (ACh) chloride, atropine (generalized muscarinic antagonist), mecamylamine hydrochloride (MCA, generalized nAChR antagonist), α-conotoxin MII (α-CT, α3β2- and β3-nAChR antagonist), methyllycaconitine citrate (MLA, α7-nAChR antagonist), and (±)-vesamicol hydrochloride (VAChT antagonist) were purchased from Tocris (Ellisville, MO). Human IGF-II was obtained from Millipore, Temecula, CA.

VAChT, AChE polyclonal antibodies and human sigma receptor monoclonal antibody were obtained from Santa Cruz Biotechnology, Santa Cruz, CA. CHT1 polyclonal and ChAT monoclonal antibodies were obtained from Millipore Inc. Phospho-Akt (Thr308), Phospho Akt (Ser473) and total Akt polyclonal antibodies were obtained from Cell Signaling Inc (Danvers, MA). HA monoclonal antibody was purchased from Covance (Princeton, NJ). The secondary donkey-anti-rabbit, rabbit-anti-mouse antibodies were obtained from Thermo Scientific, Rockford, IL.

The plasmid pcDNA3-HA-Akt-CA (T308D, S473D) (Addgene plasmid 142571) was a kind gift from Dr. Jim Woodgett, University of Ontario.

Cell lines and Cell Culture

The human squamous cell carcinoma of the lung (SCC-L) cell line NCI-H520 (hereafter referred to as H520) was obtained from American Type Culture Collection (Rockville, MD). H520 cells were grown in RPMI-1640 medium (Mediatech, Inc, Manassas, VA) supplemented

with 2 mM glutamine, 100 U/mL penicillin, 50 µg/mL streptomycin, and 10% FBS. The cells were incubated at 37°C in 5% CO_2. The H520 cells were authenticated by the ATCC Cell Authentication service in October 2012. They used Short Tandem Repeat (STR) profiling, for authentication of these cells and the results are summarized in Supplementary Figure 1.

Primary human pulmonary alveolar epithelial cells (HPAEpiCs) were obtained from ScienCell (Carlsbad, CA) and cultured in alveolar epithelial cell medium (AEpiCM) supplemented with 5% FBS. All experiments with the HPAEpiCs were performed between passage numbers 3-7. HPAEpiCs were characterized by ScienCell Inc. by immunostaining for specific markers. A certificate of analysis was provided.

Lysates and Western Blotting

Lysates for each cell line were made using the NP-40-based lysis protocol (1, 2). Cells were harvested and washed three times with ice cold 1X PBS. Cells were then lysed with M2 lysis buffer (20 mM Tris, pH 7.6, 0.5% NP-40, 250 mM NaCl, 3 mM EGTA, 3 mM EDTA, 4 µM DTT, 5 mM PMSF, 1 mM sodium fluoride, 1 mM sodium orthovanadate, 25 µg/ml leupeptin, 5 µg/ml pepstatin, 5 µg/ml aprotinin, 25 µg/ml trypsin-chymotrypsin inhibitor). Seventy five microliters of lysis buffer was added for every 20 µL of packed cell volume. The lysate was rotated at 4°C for 30 minutes and subsequently spun at 15000g for 15 minutes at 4°C. The supernatant was collected for further analysis. The protein concentration of the lysate was measured using a Bradford Reagent (Bio-Rad Labs, Hercules, CA, USA). Two hundred microgram aliquot of the protein was run on a 10% SDS-PAGE gel and transferred onto nitrocellulose membranes (Bio-Rad Labs).

The relative expression of the indicated proteins was analyzed by western blotting. The signal obtained in the western blot experiments was detected by the SuperSignal West Dura Extended Duration Substrate (Pierce Biotechnologies, Rockford, IL, USA). The results of the

western blotting assays were quantitated by ImageJ 1.46p (National Institutes of Health, Bethesda, MD, USA).

BrdU Proliferation Assays

BrdU assays were used to examine the proliferative effects of ACh on A549 or H358 cells (3, 4). A549 cells were plated in 8-well chamber slide at a density of 10,000 cells/well in SF-RPMI. After overnight incubation, the medium was aspirated and replaced with SF-RPMI containing ¼ growth factors (referred to hereinafter as SF-RPMI-R) for 24-hours. After 24-hours, these cells were treated with varying concentrations of ACh, and incubated for 48-hours at 37°C. The rate of BrdU incorporation in cells was measured by the BrdU Labeling and Detection Kit II (Roche Applied Science, Indianapolis, IN, USA) according to manufacturer's instructions. The magnitude of BrdU incorporation in control cells was considered to be equal to 1, and the BrdU incorporation observed in ACh-treated cells was calculated as fold-increase relative to the control cells. The assay was completed in duplicate, and the whole experiment was performed two independent times.

BrdU assays were also performed to examine the effect on vesamicol on EGF-induced proliferation as well as IGFII-induced proliferation in human BAC cells. A549 cells were seeded in 8-well chamber slides as described above. Subsequently the cells were rendered quiescent in serum-free RPMI for 24-hours. After 24-hours, cells were treated with 10ng/ml EGF (or 20ng/ml IGF-II) in the presence or absence of 50 µM vesamicol for 36-hours at 37°C. The concentrations of EGF and IGF-II were selected from previous publications. The BrdU assay was performed as described above.

MTT Assay

A549 or H358 cells were plated in 96-well plates at a density of 2500 cells/well in SF-RPMI. After overnight incubation at 37°C, the medium was replaced with SF-RPMI-R. Cells were treated with 100 nM nicotine in the presence or absence of varying concentrations of vesamicol for 48-hours. After 48-hours, the MTT assay was performed as described previously (1, 4). The experiment was performed two independent times with three replicates in each experiment for each cell line.

siRNA Transfection Assays

Chemically synthesized, double stranded VAChT-siRNA and Sigma receptor-siRNA (sigmaR-siRNA) were purchased from Santa Cruz Biotechnologies, Inc. The transfection experiments were performed in A549 and H358 cells. The transfection of 75 nM VAChT-siRNA or control-siRNA was performed by using Oligofectamine reagent (Invitrogen, Carlsbad, CA, USA), according to the manufacturer's protocol (1, 2). Eighteen hours post-transfection, the cells were incubated in SF-RPMI-R media for 24 hours, after they were treated with 100 nM nicotine in the presence or absence of 50 μM vesamicol for 48 hours. The effect of VAChT-siRNA or Sigma-R-siRNA on the apoptotic activity of vesamicol was measured by the caspase-3 activity kit (Millipore). A non-targeting siRNA sequence (Santa Cruz Biotechnologies, Inc.) was used as a control for the transfection experiments (5, 6) (1). The entire experiment was repeated with a second VAChT-siRNA (Ambion, Grand Island, NY, USA). Each transfection was performed in duplicate, and the entire assay was performed 2 independent times.

The efficiency of VAChT-siRNA transfection was assessed by the VAChT ELISA kit (Antibodies Online) in A549 and H358 cells. Western blotting experiments were performed to examine the expression of the Sigma-receptor after siRNA transfection (1). The results of the western blotting assays were quantitated by ImageJ 1.46p (National Institutes of Health, Bethesda, MD, USA).

Transient Transfection Assays

A549 or H358 cells were cultured to 50-70% confluence in SF-RPMI medium and transfected with 4 µg of pcDNA3-Akt-constitutively active (pcDNA3-HA-Akt-CA) using Fugene HD transfection reagent (Roche Applied Sciences, Indianapolis, IN), according to the manufacturer's protocols (2, 5). Cells transfected with the empty vector pcDNA3 were used as a control (mock transfected). After overnight incubation, the cells were rendered quiescent by incubating them in SF-RPMI-R medium for 24 hours. Subsequently, the cells were treated with 100 nM nicotine in the presence or absence of 50 μM vesamicol for 48 hours at 37°C. Lysates were made and the apoptotic activity of vesamicol was measured by the caspase-3 activity kit (EMD Millipore Corporation). The experiment was performed two independent times with two replicates in each experiment. The over-expression of the plasmid after transfection was analyzed by western blotting. The results of the western blotting assays were quantitated by ImageJ 1.46p (National Institutes of Health, Bethesda, MD, USA).

	A549 ATCC Cat. No. CCL-185		NCI-H520 ATCC Cat. No. HTB-182		NCI-H358 ATCC Cat. No. CRL-5807	
	Database Profile	Submitted Sample	Database Profile	Submitted Sample	Database Profile	Submitted Sample
D5S818	11	11	12,13	12,13	10,12	10,12
D13S317	11	11	10,11	10,11	8,12	8,12
D7S820	8,11	8,11	8,12	8,12	10,11	10,11
D16S539	11,12	11,12	8,13	8,13	12,13	12,13
vWA	14	14	18,19	18,19	17	17
THO1	8,9.3	8,9.3	10	10	6	6
AMEL	X,Y	X,Y	X	X	X,Y	X,Y
TPOX	8,11	8,11	8	8	8,9	8,9
CSF1P0	10,12	10,12	10	10	11,12	11,12
% Match	100 %		100 %		100 %	

Figure S1. A summary of the cell line authentication data for A549, H520 and H358 cells was obtained from the ATCC Cell Line Authentication service. They used Short Tandem Repeat (STR) profiling, for authentication of these cells. As indicated in the last row, the profile of the cell lines used in this study were a 100% match for A549, NCI-H520 and NCI-H358 profile described in the ATCC database.
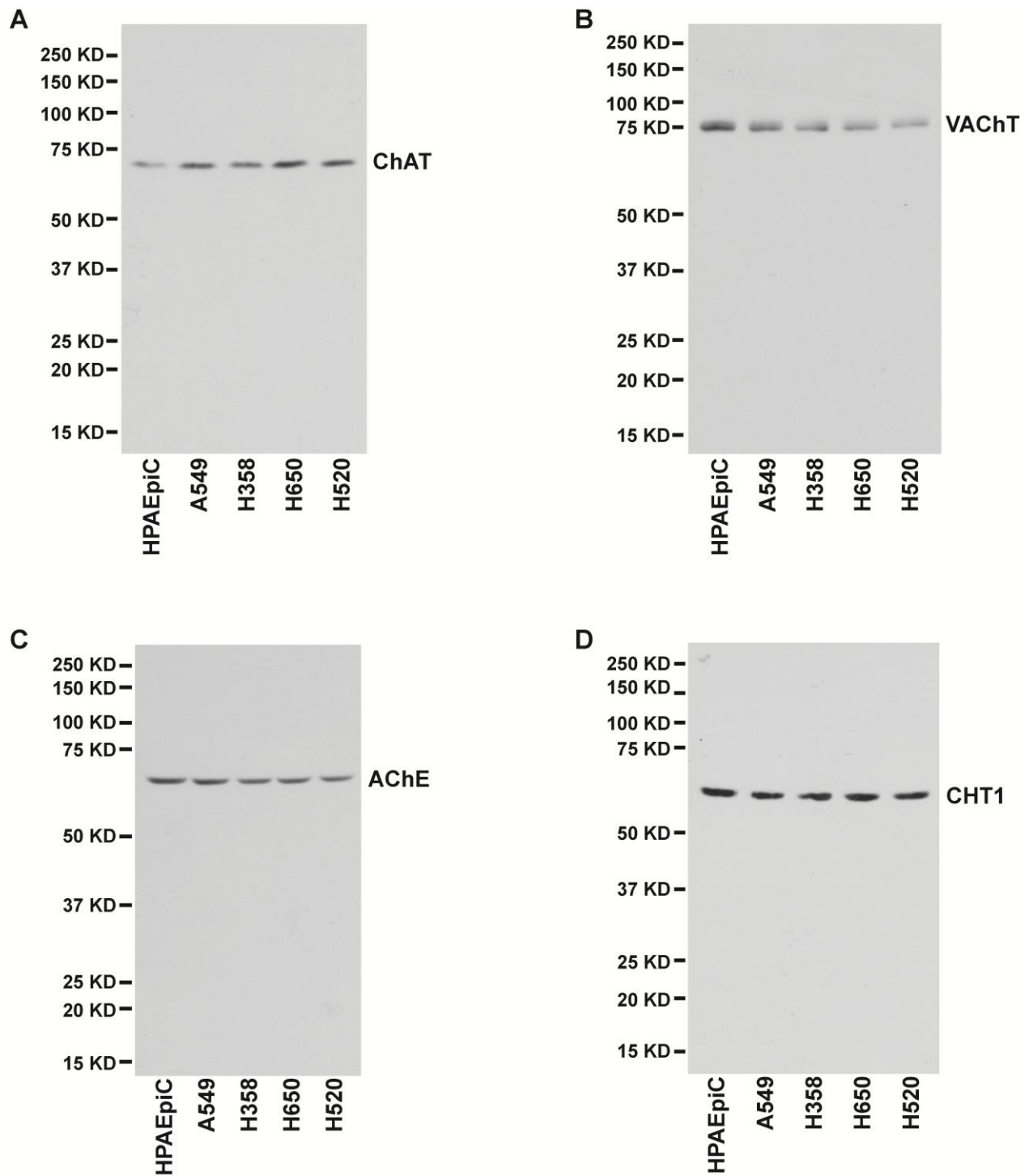
Figure S2. Full screen western blots (corresponding to Figure 1B) for the cholinergic proteins namely ChAT, VAChT, AChE and CHT1 in normal human pulmonary alveolar epithelial cells

(HPAEpiCs) and human BAC cell lines. The human SCC-L cell line H520 was used as the positive control for the immunoblotting experiments.
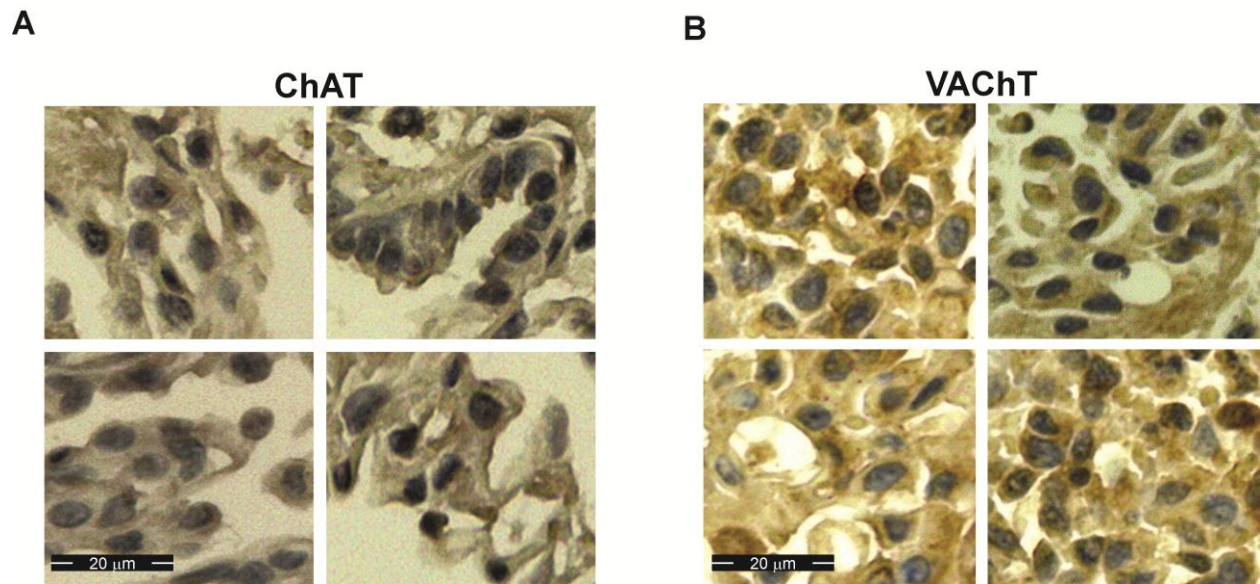
Figure S3. Normal lung tissues contain ChAT and VAChT. Immunohistochemical staining of normal lung TMA reveals the presence of ChAT and VAChT on normal lung tissues isolated from patients. The normal lung tissue microarray (TMA) was stained with ChAT monoclonal antibody and VAChT polyclonal antibody, used in the western blotting experiments outlined in Figure S2. The slides were counterstained with hemotoxylin. The staining of both ChAT and VAChT was observed to be cytoplasmic, adjacent to the hemotoxylin-stained dark nuclei in the tissue sample. This TMA contained 20 normal lung tissue samples. Photographs of four representative samples are shown above. Scale bar = 20µm
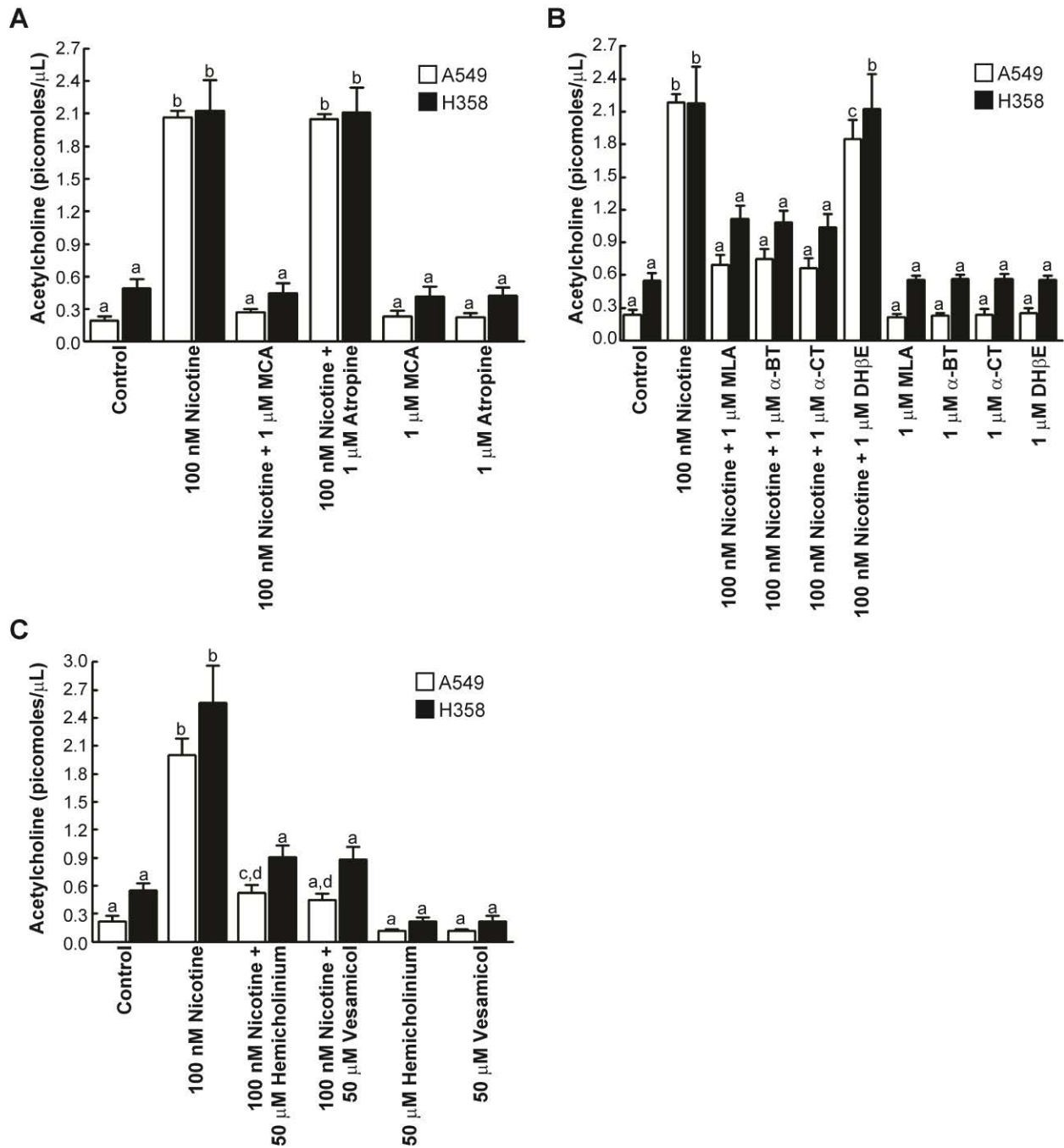
Figure S4. Nicotine-induced ACh production is mediated by $\alpha 7$-, $\alpha 3\beta 2$- and $\beta 3$-containing-nAChR subunits and requires VAChT and CHT1. **A.** Nicotine-induced ACh production was inhibited by 1 µM of the generalized nAChR antagonist, mecamylamine (MCA), but was unaffected by 1 µM of the muscarinic receptor antagonist atropine in A549 and H358 cells. The treatment of A549 and H358 human BACs with MCA or atropine alone had little to no effect on

ACh levels. **B.** The treatment of A549 and H358 human BAC cells with 1 μM of methyllylcaconitine (MLA), α-bungarotoxin (α-BT) and α-conotoxin (α-CT) MII ablated nicotine-induced ACh production, whereas DHβE (α3β2 and α4β2 nAChR antagonist) had little to no effect. **C.** Vesamicol and hemicholinium ablated nicotine-induced ACh production in A549 and H358 human BACs. Each sample was analyzed in triplicate. Data represent mean $\pm$ SEM from two independent experiments. Results indicated by a different letter are significantly different (P < 0.05*).*
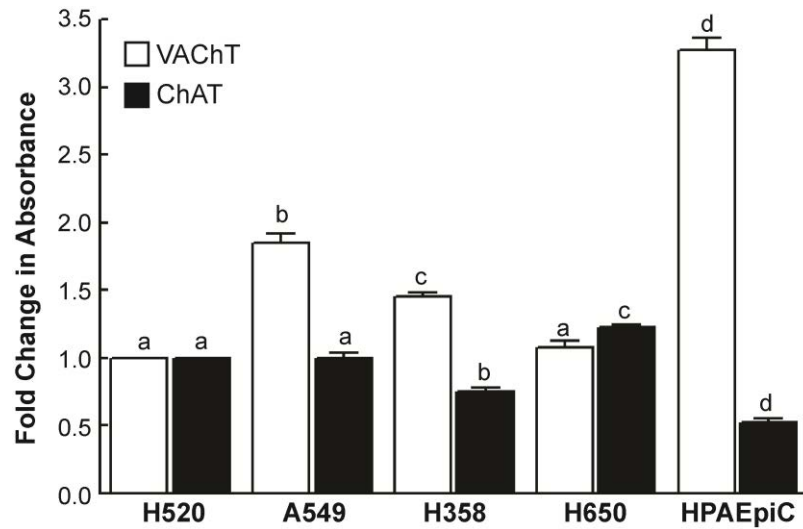
Figure S5. VAChT and ChAT are expressed on human BACs. ELISA assays were used to measure the relative levels of ChAT and VAChT on A549, H358, H650 human BAC cells and HPAEpiC normal lung cells. H520 human SCC-L cells were used as the positive control for the assay. The absorbance obtained in H520 lysates was taken as 1 and the absorbance values in the other cell lines were calculated as fold changes over H520. Each sample was assayed in duplicate and the entire experiment was repeated twice. Data represent mean $\pm$ SEM from two independent experiments. Results indicated by a different letter are significantly different ($P <$ 0.05).
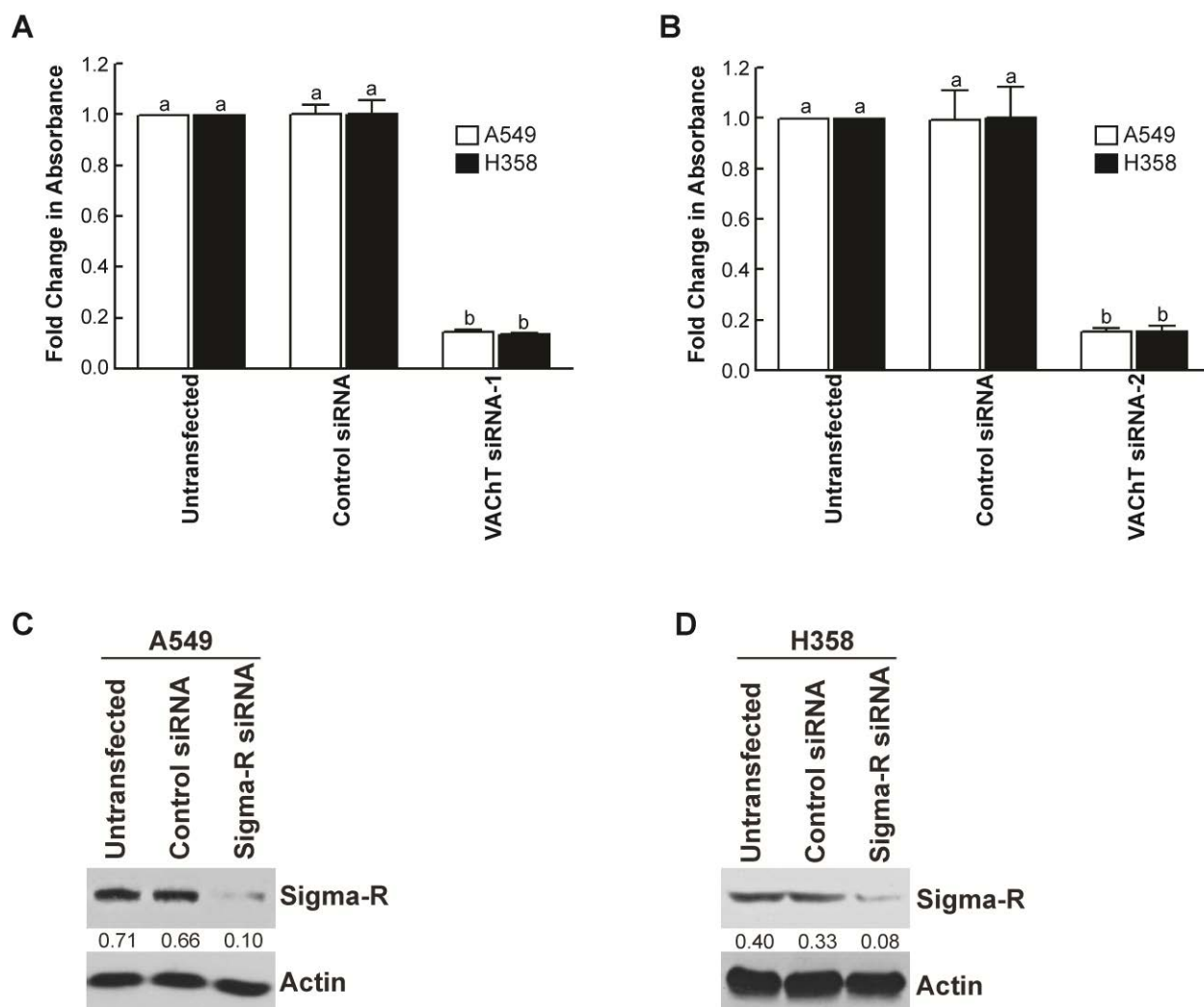
Figure S6. The transfection of VAChT-siRNA and sigma-R-siRNA suppresses the expression of these proteins in human BACs. ELISA assays show that transfection of VAChT-siRNA-1 and VAChT-siRNA-2 decrease the expression of VAChT in A549 cells **A**. and H358 cells **B**. Each sample was assayed in duplicate and the entire experiment was repeated twice. Data represent mean $\pm$ SEM from two independent experiments. Results indicated by a different letter are significantly different ($P < 0.05$).Western blotting experiments demonstrate that the level of sigma-receptor is decreased after siRNA transfection in A549 cells **C**. and H358 cells **D**. The western blot was quantitated using NIH ImageJ 1.46p.
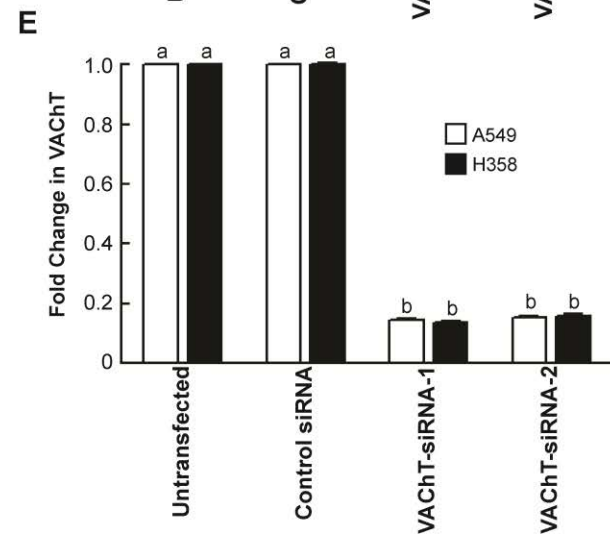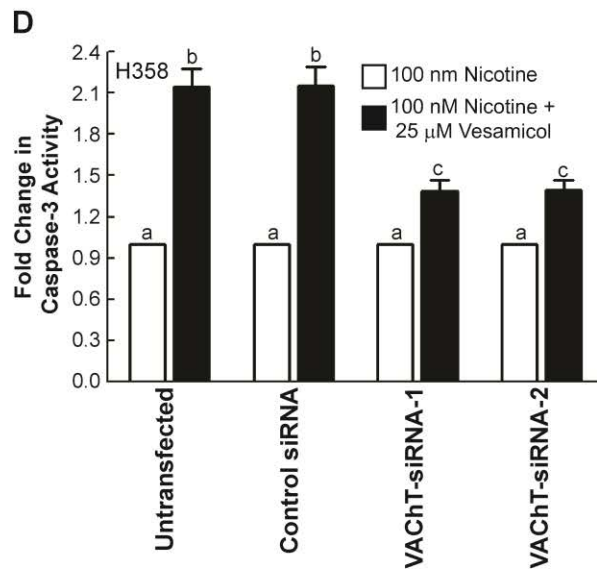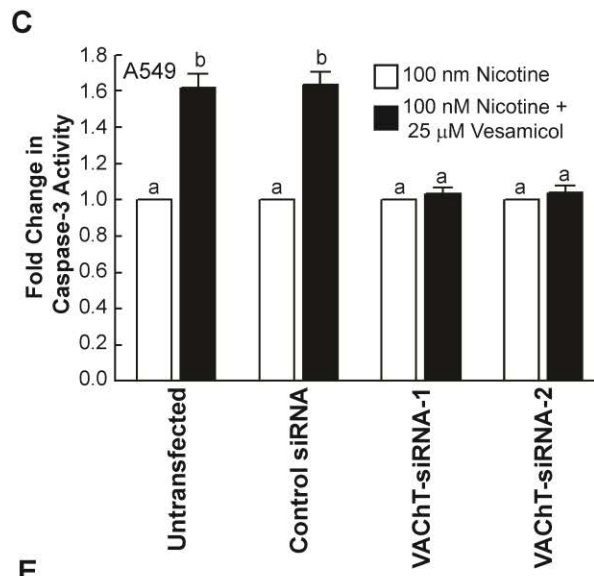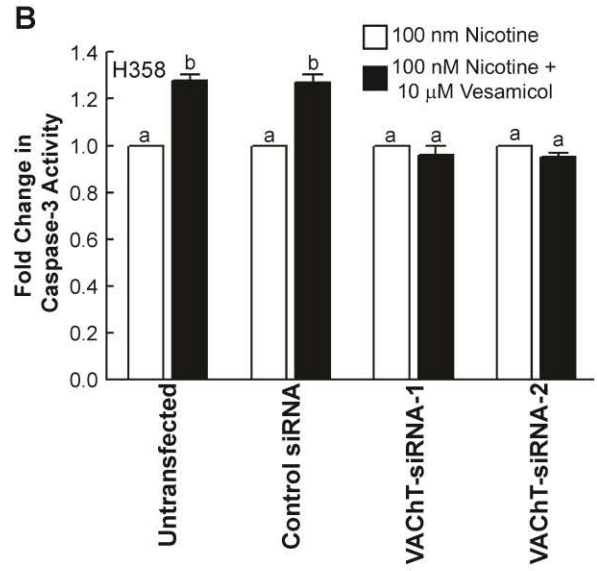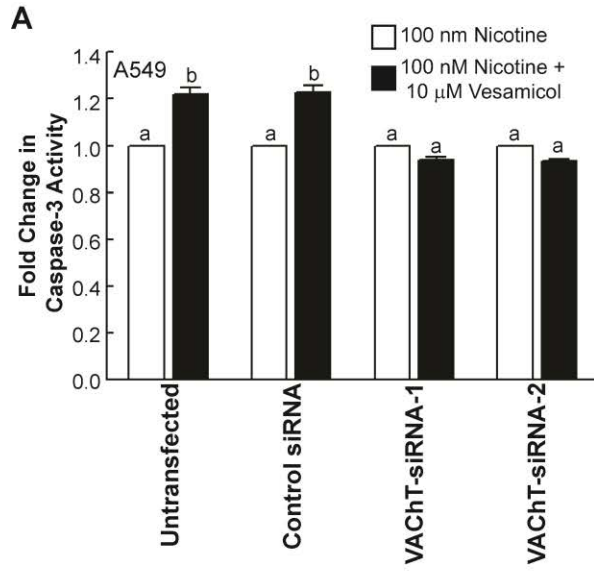
Figure S7. **A**. The pro-apoptotic activity of 10µM vesamicol in nicotine-treated A549 cells was abrogated by two independent VAChT-siRNA , namely VAChT-siRNA-1 and VAChT -siRNA-2. The transfection of a non-targeting control-siRNA had no effect on vesamicol-induced apoptosis in A549 cells. Both the VAChT-siRNA had no effect on only nicotine-treated A549 cells (white bars). **B.** The experiment was repeated in H358 human BAC cells and similar results were obtained. **C.** The apoptotic effects of 25µM vesamicol in nicotine-treated A549 cells was reversed by VAChT-siRNAs , namely VAChT-siRNA-1 and VAChT -siRNA-2. The VAChT-siRNAs did not have any effect on nicotine-treated A549 cells (white bars). **D.** The experiment was also performed in H358 cells and similar results were obtained. **E.** ELISA assays show that the transfection of both the VAChT-siRNAs caused robust suppression of VAChT levels on A549 and H358 cells. Data represent mean $\pm$ SEM from two independent experiments. Results indicated by a different letter are significantly different ($P < 0.05$).
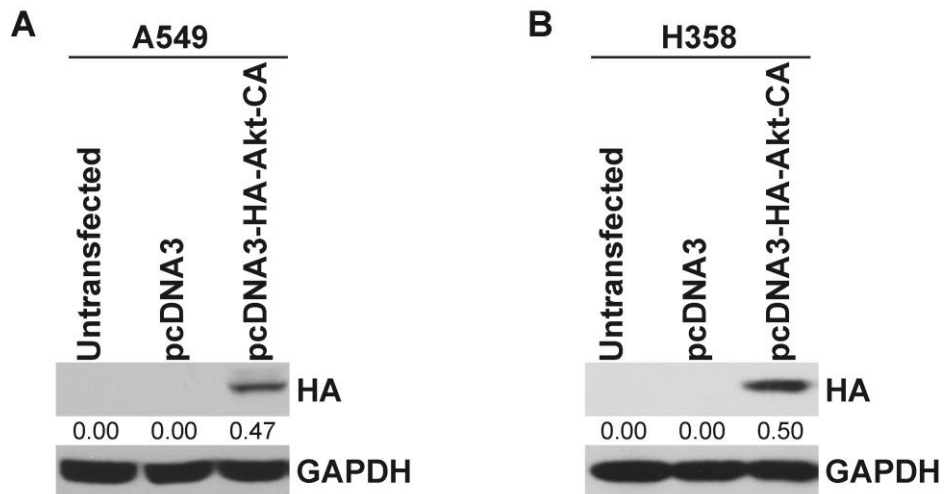
Figure S8. Western blot analysis shows that pcDNA3-HA-Akt-CA is overexpressed upon transfection in A549 cells **A**. and H358 cells **B**. The transfection was performed in duplicate and the whole experiment was repeated twice. The western blot was quantitated using NIH ImageJ 1.46p.

References

1. Brown KC, Witte TR, Hardman WE, Luo H, Chen YC, Carpenter AB, et al. Capsaicin displays anti-proliferative activity against human small cell lung cancer in cell culture and nude mice models via the E2F pathway. PLoS One. 2010;5:e10243.

2. Dasgupta P, Rizwani W, Pillai S, Davis R, Banerjee S, Hug K, et al. ARRB1-Mediated Regulation of E2F Target Genes in Nicotine-Induced Growth of Lung Tumors. J Natl Cancer Inst. 2011;103:317-33.

3. Dasgupta P, Rastogi S, Pillai S, Ordonez-Ercan D, Morris M, Haura E, et al. Nicotine induces cell proliferation by beta-arrestin-mediated activation of Src and Rb-Raf-1 pathways. J Clin Invest. 2006;116:2208-17.

4. Dasgupta P, Sun J, Wang S, Fusaro G, Betts V, Padmanabhan J, et al. Disruption of the Rb--Raf-1 interaction inhibits tumor growth and angiogenesis. Mol Cell Biol. 2004;24:9527-41.

5. Brown KC, Lau JK, Dom AM, Witte TR, Luo H, Crabtree CM, et al. MG624, an alpha7-nAChR antagonist, inhibits angiogenesis via the Egr-1/FGF2 pathway. Angiogenesis. 2012;15:99-114.

6. Dom AM, Buckley AW, Brown KC, Egleton RD, Marcelo AJ, Proper NA, et al. The alpha7-nicotinic acetylcholine receptor and MMP-2/-9 pathway mediate the proangiogenic effect of nicotine in human retinal endothelial cells. Invest Ophthalmol Vis Sci. 2011;52:4428-38.